EUROPEAN COMMISSION

Community Research

SEVENTH FRAMEWORK PROGRAMME

ARCHER

Collaborative Project (CP)

Co-funded by the European Commission under the Euratom Research and Training Programme on Nuclear Energy within the Seventh Framework Programme

Grant Agreement Number : 269892

Start date : 01/02/2011 Duration : 48 Months

www.archer-project.eu

Advanced Reactor for Cogeneration of Heat & Electricity-R&D

Corrosion mechanism of Fuel coatings and implication for overall spent fuel performance

Authors : AIT CHAOU Abdel (ARMINES) , Abdelouahed Ait Chaou, Abdesselam Abdelouas, Gokhan Karakurt and Bernd Grambow

ARCHER - Contract Number: 269892
Advanced High-Temperature Reactors for Cogeneration of Heat and Electricity R&D
EC Scientific Officer: Dr. Panagiotis Manolatos

Document title	Corrosion mechanism of Fuel coatings and implication for overall spent fuel performance
Author(s)	AIT CHAOU Abdel , Abdelouahed Ait Chaou, Abdesselam Abdelouas, Gokhan Karakurt and Bernd Grambow
Number of pages	40
Document type	Deliverable
Work Package	WP 33
Document number	D33.11
Issued by	NRG
Date of completion	08/01/2014
Dissemination level	Confidential, only for members of the consortium (including the Commission Services).

Summary

High-Temperature Reactor fuels consist of the bistructural-isotropic (BISO) or tristructural-isotropic (TRISO) coated particles embedded in a graphite matrix. Geological disposal may be envisaged for spent fuel management. In this framework we investigated the alteration of BISO (with pyrolytic carbon) and TRISO (with SiC) particles under geological conditions simulated by temperatures of 50 and 90?C and a synthetic groundwater. Solid state (scanning electron microscopy (SEM), micro-Raman spectroscopy, electron probe microanalyses (EPMA) and X-ray photoelectron Spectroscopy (XPS)) and solutions analyses (ICP-MS, ionique chromatography (IC)) showed the clear oxidation of both pyrolytic carbon and SiC at 90?C with the formation of SiO2 and a clay-like Mg-silicate under air while under reducing conditions (H2/N2 atmosphere) SiC and pyrolytic carbon were highly stable after a few months of alteration. At 50?C regardless the redox conditions the alteration of the coatings was minor. In conclusion, due to their high stability in reducing conditions HTR fuels disposal in deep geological rocks may constitute a good solution for their management.

Approval

Date	By
26/06/2014	Abdelouas ABDESSELAM
07/07/2014	Mathias LAURIE
07/07/2014	Steven KNOL

Distribution list

Name	Organisation	Comments
P. Manolatos	EC DG RTD	Through the EC participant portal
All beneficiaries	ARCHER	Through the private online workspace

Final Report
SP3: Fuel & Fuel Cycle
WP33 – D33.11

Corrosion mechanism of Fuel coatings and implication for overall spent fuel performance: Alteration of BISO and TRISO particles in groundwater

A. A. Ait Chaou, A. Abdelouas, B. Grambow, G. Karakurt,

December 2013

ARCHER project – Contract Number: 269892
Advanced High-Temperature Reactors for Cogeneration of Heat and Electricity R&D

EC Scientific Officer: Dr. Panagiotis Manolatos

Document title	Corrosion mechanism of Fuel coatings and implication for overall spent fuel performance
Author(s)	A. Ait Chaou, A. Abdelouas, B. Grambow, G. Karakurt (SUBATECH Laboratory)
Number of pages	38
Document type	Deliverable
Work Package	SP3 – WP33
Document number	SP3 – WP33 - D33.11 – Final Report
Issued by	SUBATECH
Date of completion	08/01/2014
Dissemination level	Restricted to the partners of the ARCHER project

Summary

This document is the final report of the archer project SP3 – WP33 - D33.11: Corrosion mechanism of Fuel coatings and implication for overall spent fuel performance (Alteration of BISO and TRISO particles in groundwater).
High-Temperature Reactor fuels consist of the bistructural-isotropic (BISO) or tristructural-isotropic (TRISO) coated particles embedded in a graphite matrix. Geological disposal may be envisaged for spent fuel management. In this framework we investigated the alteration of BISO (with pyrolytic carbon) and TRISO (with SiC) particles under geological conditions simulated by temperatures of 50 and 90°C and a synthetic groundwater. Solid state (scanning electron microscopy (SEM), micro-Raman spectroscopy, electron probe microanalyses (EPMA) and X-ray photoelectron Spectroscopy (XPS)) and solutions analyses (ICP-MS, ionique chromatography (IC)) showed the clear oxidation of both pyrolytic carbon and SiC at 90°C with the formation of SiO_2 and a clay-like Mg-silicate under air while under reducing conditions (H_2/N_2 atmosphere) SiC and pyrolytic carbon were highly stable after a few months of alteration. At 50°C regardless the redox conditions the alteration of the coatings was minor. In conclusion, due to their high stability in reducing conditions HTR fuels disposal in deep geological rocks may constitute a good solution for their management.

Approval

Rev.	Short description	First author	WP Leader	SP leader	Coordinator
0	-	Abdelouahed Ait Chaou and Abdesselam Abdelouas (SUBATECH) 08/01/2014	Bernd Grambow	Mathias Laurie	Name (org) ../../..

Distribution list

Name	Organisation	Comments
P. Manolatos	EC DG RTD	
All technical participants	ARCHER	
Steering Committee members	ARCHER	

Table of contents

1. Objective

Study the alteration of BISO and TRISO (without external pyrolytic carbon) particles in synthetic Callovo-Oxfordian water (COX water) at 50 and 90°C. The COX water is the French reference HLW disposal site.

2. Introduction

TRISO particle fuel is envisaged to be used in very high temperature (VHTR) gas-cooled reactors. TRISO-coated fuels (900 µm diameter) are composed of a heavy metal (e.g., uranium, plutonium, thorium, etc.) oxide or mixed oxide/carbide fuel kernel (500 µm diameter) coated with four layers of three isotropic materials. The four layers are a porous carbon layer (buffer, 95 µm), followed by three sequential layers: a dense inner pyrolytic carbon layer (IPyC, 40 µm), a silicon carbide layer (SiC, 35 µm), and a dense outer pyrolytic carbon layer (OPyC, 40 µm). The role of the SiC layer is critical, since it does not only provide the TRISO particle with structural integrity but also retains fission products and serves as a critical barrier at elevated temperatures. In addition to SiC, other carbides such as ZrC with competitive superior performance are being developed for TRISO coatings.

Recently the properties of dense pyrolytic carbon have been identified as one of the limitations in achieving higher burn-ups in the fuel particle [1]. One of the first applications of PyC was in the production of BISO and TRISO-coated fuel particles. It has been shown that without the proper microstructure and mechanical properties of pyrolytic carbon, the stresses or structural changes introduced in this coating could result in the total failure of the coated particle [2]. Since properties such as Young's modulus and thermal conductivity are controlled by the microstructure of pyrolytic carbon [3].

A chemical vapour deposition (CVD) technique is one of the most familiar gas phase reaction methods for the synthesis of highly crystalline, stoichiometric, high-purity β-SiC for TRISO particles [4, 5].

A TRISO fuel particle is like a pressure vessel that contains fission products. Like any other pressure container, when it corrodes significantly it will erupt. This eruption will release gaseous fission products and allow the other radioactive material to be available for transport out of the particle. The SiC and pyrocarbon layers act like a pressure vessel within the TRISO fuel. Corrosion of these layers is caused by oxidation with air and water at the outer surface.

Chemical properties of silicon carbide and pyrocarbon

The chemical bonding in SiC is not only covalent but also slightly ionic due to the differential electronegativity between silicon and carbon. The only stable compound in the system Si-C is therefore obtained at the stoichiometric composition.

The superior mechanical properties, high thermal conductivity, low thermal expansion, thermal shock resistance and chemical inertness of SiC are important for its use in the immobilization of nuclear waste.

In a geologic repository, SiC coated waste forms or TRISO fuel may be subjected to oxic corrosion in water at temperatures below 200 °C due to remains of air introduced during site construction but for long-term duration anaerobic and reducing conditions will prevail assuring a better stability for the waste form. Oxidation rates of SiC in dry and moist air under these repository conditions are minimal, even after a million years [6].

Early studies in Germany on the dissolution of TRISO-coated particles in brine at temperatures up to 150 °C and pressures of 300 atmospheres indicated no evidence for corrosion over times exceeding 4 years [7].

Recent studies on the corrosion rates of unirradiated and neutron-irradiated SiC in different simulated ground waters over a range of temperatures revealed no significant long-term effect of irradiation on corrosion behaviour [8, 9]. The mechanisms and rates of corrosion for SiC in different aqueous media under conditions relevant to geologic repositories have also been recently reviewed by McEachern et al. [6].

Fachinger et al. [8] studied the graphite, pyrocarbon, SiC and fuel kernels corrosion in aqueous phases from salt, granite, and clay host rock at different temperature and pH. Results of corrosion rates and lifetime of non-irradiated SiC and pyrocarbon are summarized in table 1 and 2 [8]. The temperature is one of the most important parameters determining the corrosion rate. The higher the temperature in the repository, the shorter the lifetimes will be. The corrosion rate increases also with increasing pH.

The authors indicate that the formation of an oxide layer decreasing the corrosion rate over time is also possible.

Table 1

Corrosion rates of non-irradiated SiC in aqueous solutions at 50℃ and 90℃ [8]

Material	Aqueous phase	Temperature (°C)	R (g/m^2/day)	Lifetime (years)
SiC	Granite water	50	3.84E−06	6.80E+03
SiC	Granite water	90	9.64E−06	2.70E+03
SiC	Q-brine	50	7.54E−06	3.47E+04
SiC	Q-brine	90	1.68E−05	1.56E+04
SiC	Clay pore pH 9	50	8.07E−06	3.24E+04
SiC	Clay pore pH 9	90	2.30E−05	1.14E+04
SiC	Clay pore pH 12	50	1.61E−05	1.62E+04
SiC	Clay pore pH 12	90	3.70E−05	7.07E+03
SiC	Clay pore pH 3	50	4.45E−06	5.88E+04
SiC	Clay pore pH 3	90	1.09E−05	2.39E+04

Table 2
Corrosion rates of non-irradiated pyrocarbon in aqueous solutions at 90℃ [8]

Materials	Aqueous phase	Atmosphere	Temperature (°C)	R (g/m^2/day)	Lifetime (years)
Pyrocarbon	Brine 2	Oxygen	90	9.3E−08	6.1E+06
Pyrocarbon	Water	Oxygen	90	4.7E−07	1.2E+06
Pyrocarbon	Water	Air	90	3.4E−07	1.7E+06
Pyrocarbon	Brine 2	Air	90	2.2E−07	2.6E+06
Pyrocarbon	Brine 2	Argon	90	1.4E−08	4.0E+07

Corrosion data for SiC in various aqueous media are available in the range 20–360 °C [8, 9, 10, 11, 12 and 13]. In high temperature corrosion of SiC in air or oxygen-containing atmospheres a protective SiO_2 layer is formed. For experiments of corrosion of SiC in water, protective layers have typically not been observed. Examination of the aqueous corroded surface indicated local attack along grain boundaries [11].

Because reactions of SiC with water produce hydrogen ions, the reaction is affected by the aqueous media pH. It has been observed that no permanent protective layer forms in aqueous media in short-term experiments. The reaction product has been suggested to be either H_2SiO_3 or $Si(OH)_4$, both of which are soluble in liquid water [11, 12, 13].

Experimental and theoretical results indicate that the corrosion rate of SiC for all aqueous solutions increase with temperature and dissolved oxygen [11]. In general the literature indicate (1) the corrosion reactions in aqueous solutions lead to soluble silicon molecules and a permanent protective layer is not observed, (2) the corrosion rates at 50–90 °C with irradiated SiC are higher than rates with non-irradiated SiC by factors of 3–4, (3) the corrosion rates increase in the presence of gamma irradiation. Also, we can notice that though SiC is considered to be chemically inert to HCl, H_2SO_4, HF, NaOH, and a mixture of HF and HNO_3, it is subjected to corrosion in the presence of Na_2SO_4 and a mixture of Na_2CO_3 and KNO_3 [14, 15].

The objective of the present work was to study the alteration of the outer PyC layer in the BISO particles and SiC layer in the TRISO particles in clayey environment referring to the French high-level long-lived radioactive waste deep geological disposal. We focus our study on the chemical changes of the SiC and Pyrocarbon layers under oxidizing and reducing conditions, possibly encountered in disposal sites. We used experimental conditions typical for the French reference site (T°: 50-90°C; synthetic groundwater).

3. Materials and methods

3.1. Materials and samples preparation

TRISO particles simulant

A non-active TRISO particle-fuel simulant provided by AREVA NP was used, employing surrogate zirconia kernels in place of UO_2. The external pyrolytic carbon was mechanically removed to study the alteration of SiC layer in aqueous solutions.

BISO Particle Simulant

The BISO particles, with kernels of Al_2O_3 and 2 pyrolytic carbon layers, were provided by the University of Manchester. The particles were altered as they received.

3.2. Experimental

BISO and TRISO (without external pyrolytic carbon) particles were altered in synthetic Callovo-Oxfordian water (COx water) at 50 and 90°C under reducing conditions (5% H_2/N_2), characteristic of the expected French site for hosting high-level waste in France. A different number of BISO and TRISO particles were used in order to show a minimum effect of surface area to solution volume (S/V) ratio (Table 3). Additional experiments in aerobic conditions were conducted to simulate the aerobic site post-closure phase in addition to possible generation of oxidizing radicals and molecules (e.g. $OH^{\bullet}$, O_2) via water radiolysis mainly by

gamma radiations. The COx water corresponds to the water originating from the French reference high-level radioactive waste (HLW) disposal site and its composition is given in Table 4. The water was prepared by dissolving salts in deionized water with a final pH of 6.5.

Table 3
Summary and experimental conditions of studied systems.

System	Solution volume	Temperature	Atmosphere	S/V (m^{-1})	Analyses
20 BISO	37 mL	50°C	5% H_2/N_2	1.7	EDX, SEM, EPMA, ICP-MS, IC, pH
			Air	1.7	EDX, SEM, ICP-MS, CI, pH
100 BISO	37 mL	50°C	5% H_2/N_2	8.5	EDX, SEM, EPMA, ICP-MS, XPS, Raman, IC, pH
			Air	8.5	EDX, SEM, EPMA, ICP-MS, XPS, Raman, IC, pH
20 BISO	37 mL	90°C	5% H_2/N_2	1.7	EDX, SEM, EPMA, ICP-MS, Raman, IC, pH
			Air	1.7	EDX, SEM, ICP-MS, Raman, IC, pH
100 BISO	37 mL	90°C	5% H_2/N_2	8.5	EDX, SEM, EPMA, ICP-MS, XPS, Raman, IC, pH
			Air	8.5	EDX, SEM, EPMA, ICP-MS, XPS, Raman, IC, pH
30 TRISO	37 mL	50°C	5% H_2/N_2	1.8	EDX, SEM, EPMA, ICP-MS, Raman, IC, pH
			Air	1.8	EDX, SEM, EPMA, ICP-MS, IC, pH
100 TRISO	37 mL	50°C	5% H_2/N_2	7	EDX, SEM, EPMA, ICP-MS, XPS, Raman, IC, pH
			Air	7	EDX, SEM, EPMA, ICP-MS, XPS, Raman, IC, pH
30 TRISO	37 mL	90°C	5% H_2/N_2	1.8	EDX, SEM, EPMA, ICP-MS, IC, pH
			Air	1.8	EDX, SEM, EPMA, ICP-MS, Raman, IC, pH
100 TRISO	37 mL	90°C	5% H_2/N_2	7	EDX, SEM, EPMA, ICP-MS, XPS, Raman, CI, pH
			Air	7	EDX, SEM, EPMA, ICP-MS, XPS, Raman, CI, pH

The experiments were conducted in stainless steel autoclaves with Teflon liners (Fig. 1) to prevent water evaporation and exchange with atmosphere, which may promote carbon and SiC oxidation. The additional experiments under aerobic conditions were conducted in plastic serum bottles, which allowed some air diffusion at temperatures higher than 40°C. Details of experiments are listed in Table 3. For the experiments conducted in reducing conditions, after addition of COx water to the particles the autoclaves were bubbled with 5% H_2/N_2 for 5 minutes to ensure reducing conditions encountered in deep geological disposal sites.

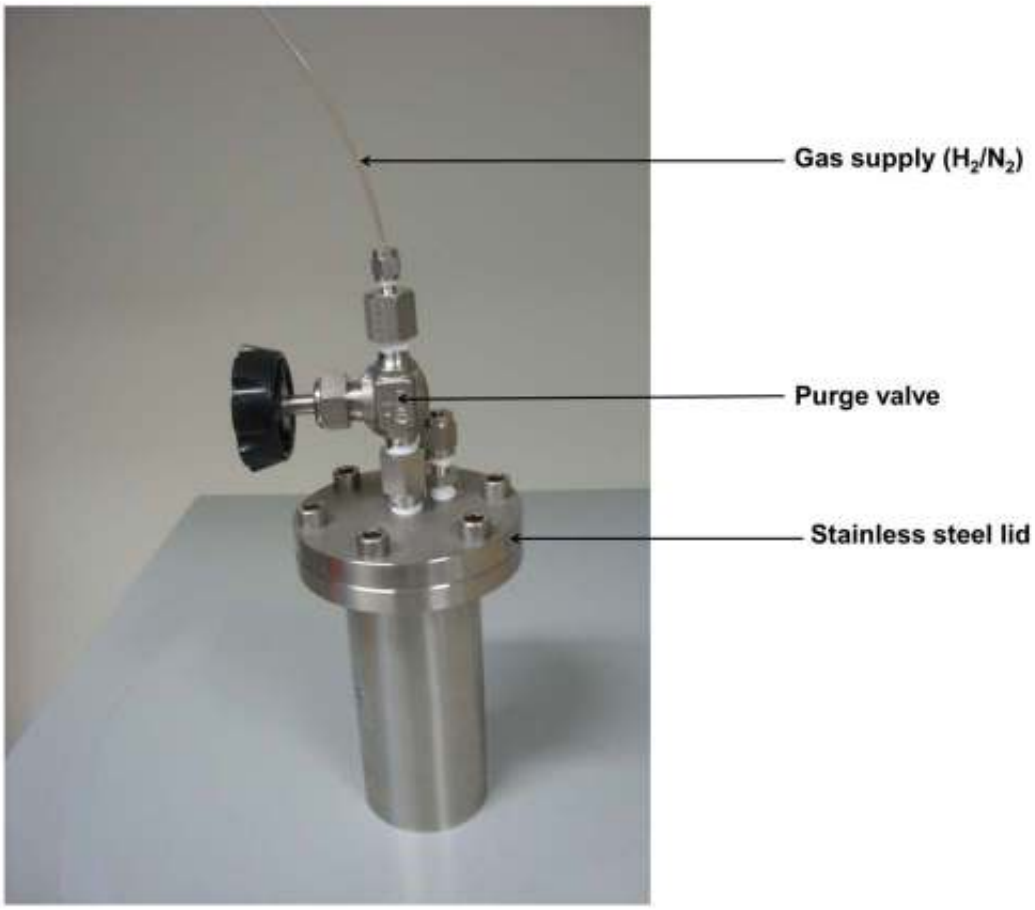

Fig. 1. *The stainless steel autoclave for alteration experiments at 50℃ and 90℃.*

Table 4

Chemical composition of synthetic COx water [16].

Element	Na^+	K^+	Ca^{2+}	Mg^{2+}	Sr^{2+}	Si
mmol/L	39	0.96	10	2.5	0.17	0.84
Element	Cl^-	SO_4^{2-}	C_{total}	Al	Fe	
mmol/L	41	10	10	8×10^{-5}	0.05	

3.3. Solid and liquid analysis

Periodic solution sampling was conducted for pH, silicon, calcium and magnesium measurements. pH measurements were performed using a pHM220 (R03 pHME01) from MeterLab. The pH meter was calibrated daily with buffers at pH 4.0, 7.0 and 10.0 and the pH tolerance is ± 0.01 pH. Silicon concentrations in the different solutions, before and after alteration, have been determined using Inductively Coupled Plasma-Mass Spectrometry (ICP-MS) with an XSERIES 2 from Thermo Scientific (sensibility limit of 0.1 ppb). Before analysis, all the solutions were diluted in HNO_3 medium (2% volume). The uncertainties associated to the measured values were estimated to be 5%. The calcium and magnesium concentrations were measured after dilution by Ion Chromatography with conductivity detection DIONEX ICS 1000. The quantification limit is 5.8×10^{-6} mol/L for Mg and 5.7×10^{-6} mol/L for Ca.

During and at the end of the alteration, solid samples (TRISO and BISO particles) were observed by Scanning Electron Microscopy (SEM) and analyzed by Energy Dispersive X-ray (EDX), micro-Raman spectroscopy, XPS (X-ray Photoelectron Spectroscopy) and Electron Probe Micro-Analysis (EPMA). In order to obtain good quality EDX and Raman patterns, cross-sections of the TRISO and BISO particles were prepared. The cross-section samples were polished with abrasive paper to 1200 grit followed by diamond paste (15, 6 and 3 µm). The analyzed thickness is about 1 µm.

The SEM analyses were done under an accelerating voltage of 15 kV (Jeol 5800). The Si (Li) detector used was equipped with a thin beryllium window that allows to detect and quantify oxygen with a good accuracy (about 1% relative error for flat sample). The Al_2O_3, pure carbon and wollastonite were used as standards for oxygen, carbon and silicon, respectively.

EPMA was used to confirm the amount of oxygen after alteration. EPMA complements EDX offering excellent peak separation, accurate trace element analysis, and optimised element detection for low and high energy X-rays to provide. The analysed thickness is about 1 µm. The EPMA experiments were made with a beam intensity of 7.6 nA and an accelerating voltage of 20 kV. The LSM80E cristal with Kα lines were used us the oxygen and carbon crystal of WDX, I_{std} = 24.3 cps/nA. For silicon we used pentaerythritol (PET) crystal, I_{std} = 550.4 cps/nA. Wafer Si, Albite and TiC were used as silicon, oxygen and carbon standards. The acquisition time for the standards was 60s for the peak and 2 × 30s for background measurement. For samples, the acquisition time was 20s for the peak and 2 × 10s for the background measurement.

The Raman spectra were recorded at room temperature in the backscattering configuration on a Jobin-Yvon-LABRAM spectrometer and a Peltier-based cooled charge coupled device (CCD) detector equipped with the

diffraction grating 600 lines/mm under a microscope (Olympus Bx41) with a 100x objective focusing the 514 nm line from an Argon ion laser. The spot size of the laser was estimated at 0.8 µm and the spectral resolution at 2 cm^{-1}. Raman measurements were carried out at very low laser power (1 mW), to avoid structural modifications or phases transitions. The Raman spectra were recorded twice in the wavenumber 100-3600 cm^{-1} region with an integration time = 600 s. Acquisition and basic treatment of spectra are made with the LabSpec (Jobin Yvon-Horiba) software. Raman measurements were carried out at very low laser power to minimize possible sample deterioration or phase transition with operating time. The analysed thickness is about 1 µm.

The O_{1s}, Si_{2p}, C_{1s} and Mg_{2p} XPS spectra are collected by an XPS apparatus with a KRATOS AXIS ULTRA electron spectrometer working in fixed analyzer transmission (FAT) mode. The source of photons is an Al monochromatic X-ray source emitting an incident X-ray beam at 1486.7 eV with a FWHM (full-width half-maximum) of 0.25 eV. The sample (BISO and TRISO particles), fixed on a metallic plate, is analyzed in a chamber under 5 x 10^{-7} Pa vacuum. The O_{1s}, Si_{2p}, C_{1s} and Mg_{2p} peaks are recorded at constant pass energy of 20 eV. The binding energy precision is better than 0.2 eV. The analysed thickness is about 5 nm.

4. Results and discussion

4.1. Pristine materials characterization

4.1.1. TRISO particles characterization

To study the SiC alteration the external pyrolytic carbon was first removed by heat treatment at 1100°C. SEM observation of heat-treated particles showed partial oxidation of SiC. Thus, we decided to mechanically remove the external carbon layer (Fig. 2a). The kernel composition was analyzed to be ZrO_2 (Fig. 2b and 2c).

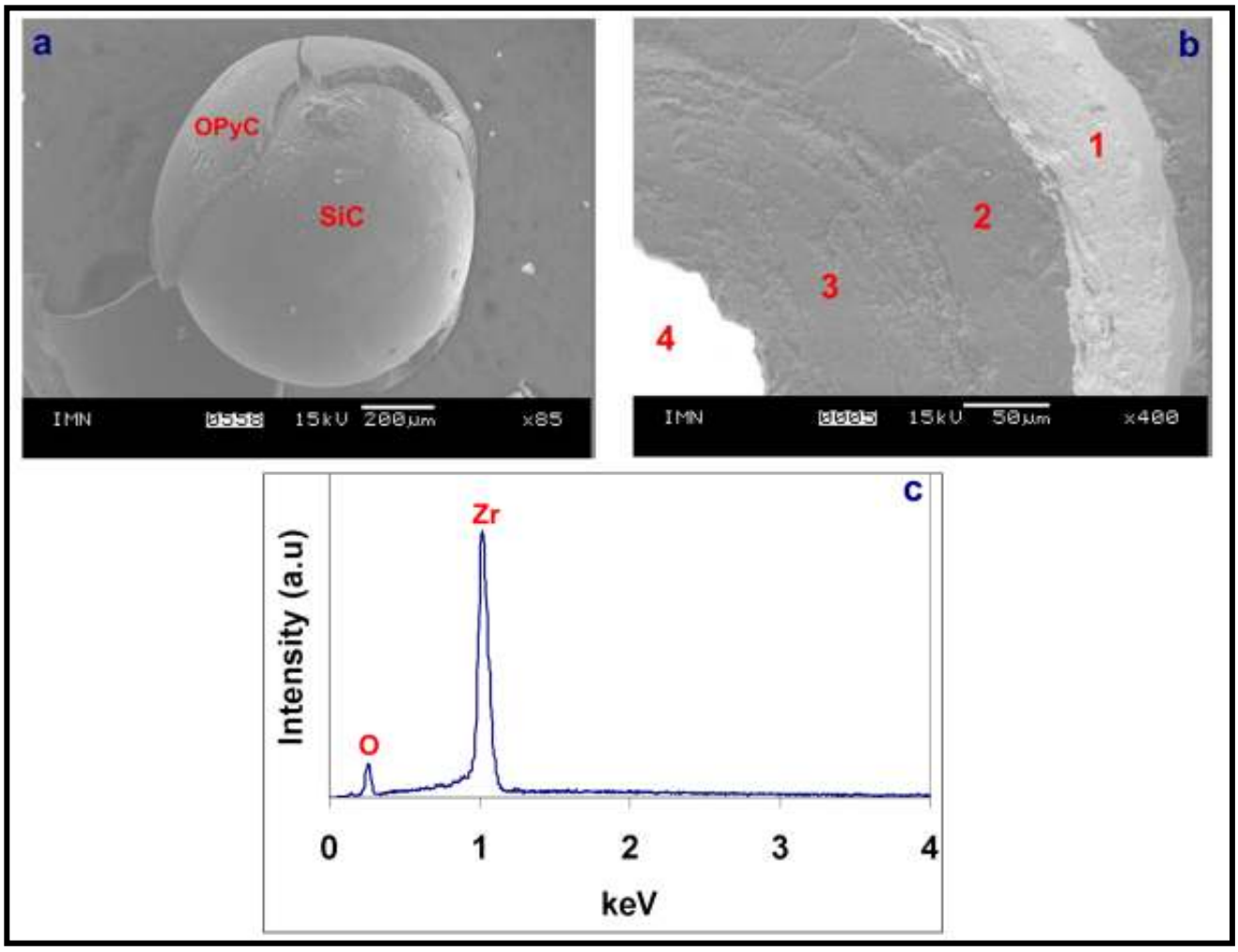

Fig. 2. *SEM micrograph of TRISO particle showing (a) external pyrolytic carbon and clean SiC layer, (b) a cross-section of a TRISO particle illustrating the tree functional layers and the central core: (1): SiC, (2): IPyC, (3): Buffer Carbon and (4): ZrO_2 core and (c) EDX spectrum of the ZrO_2 kernel of a TRISO particle.*

4.1.2. BISO particles characterization

A scanning electron microscope micrograph of a BISO particle can be seen in Fig. 3a. The chemical composition obtained by EDX shows the unique presence of carbon without oxygen (Fig.3b.). Fig. 3c shows the kernel and the 2 carbon layers. The kernel composition was analyzed to be Al_2O_3 (Fig. 3d).

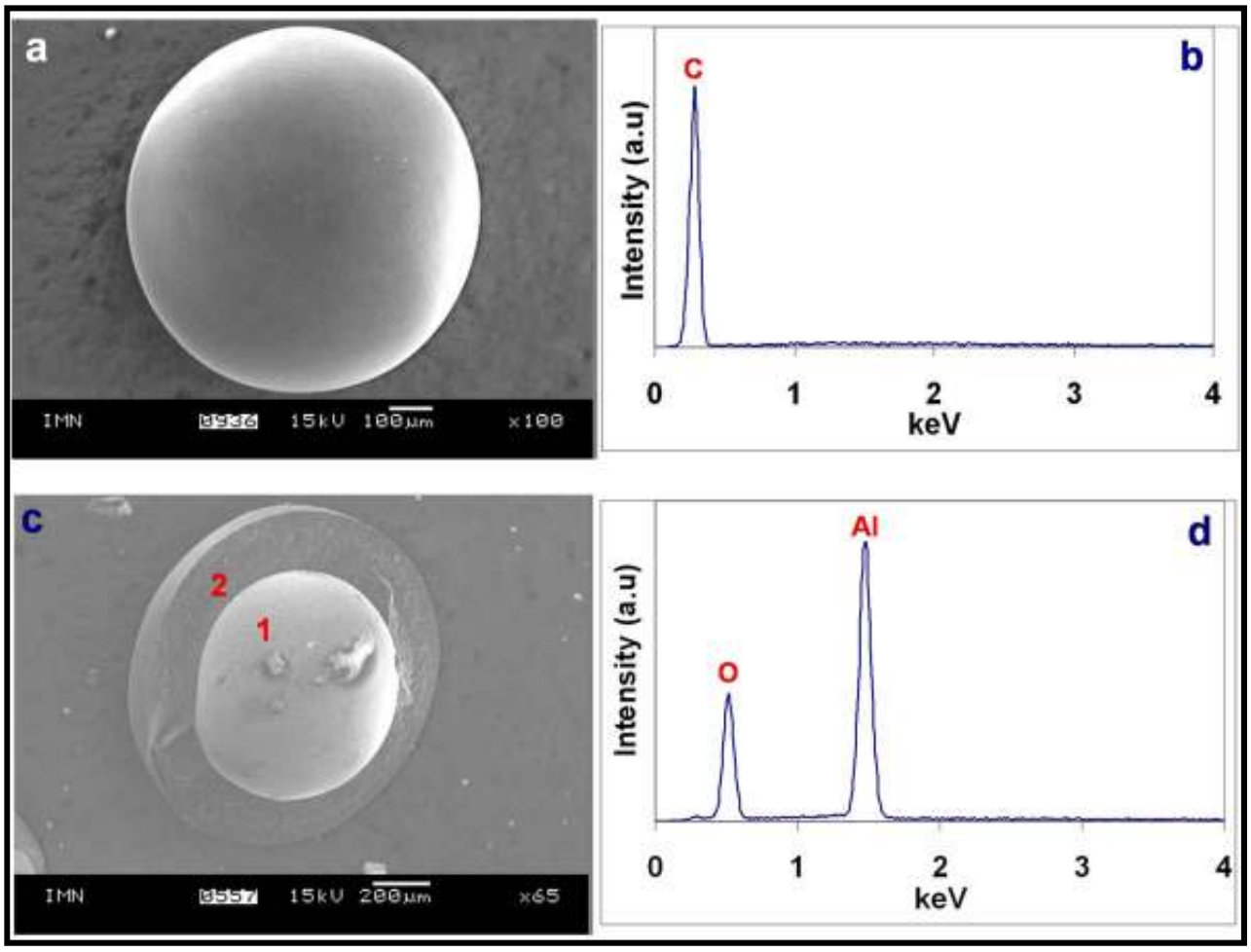

Fig. 3. *(a) SEM micrograph and (b) EDX spectrum of BISO particle surface, (c) cross section of BISO particle showing (1): Al_2O_3 kernel and (2): carbon layers, (d) EDX spectra of the Al_2O_3 kernel.*

To check the nature of pyrolytic carbon in BISO and TRISO particles we performed μ-Raman spectroscopy analysis. Fig. 4 shows the Raman spectra of the external pyrolytic carbon in the TRISO and BISO particles. The two characteristic bands are the D-band around 1340 cm^{-1} and the G-band at 1580 cm^{-1}. These bands give information on the molecular structure and chemicals bonding of carbon atoms in carbonaceous materials. The so-called G-line (the disorder band is well-known in disordered graphitic materials) and corresponds to the tangential vibration of the carbon atoms (stretching mode of the carbon-carbon bond). The second characteristic mode (D-band) is a typical sign for defective graphitic structures.

The Raman intensity of the D band (I_D) and G band (I_G) is inversely proportional to the carbon crystallize size. The D and G mode frequencies are identical for the TRISO and BISO particles and the variation in intensity ratios was close enough: I_D/I_G = 2.38 for TRISO and I_D/I_G = 2.46 for BISO. It can be concluded that the structural properties of pyrocarbon is the same in the TRISO and BISO particles.

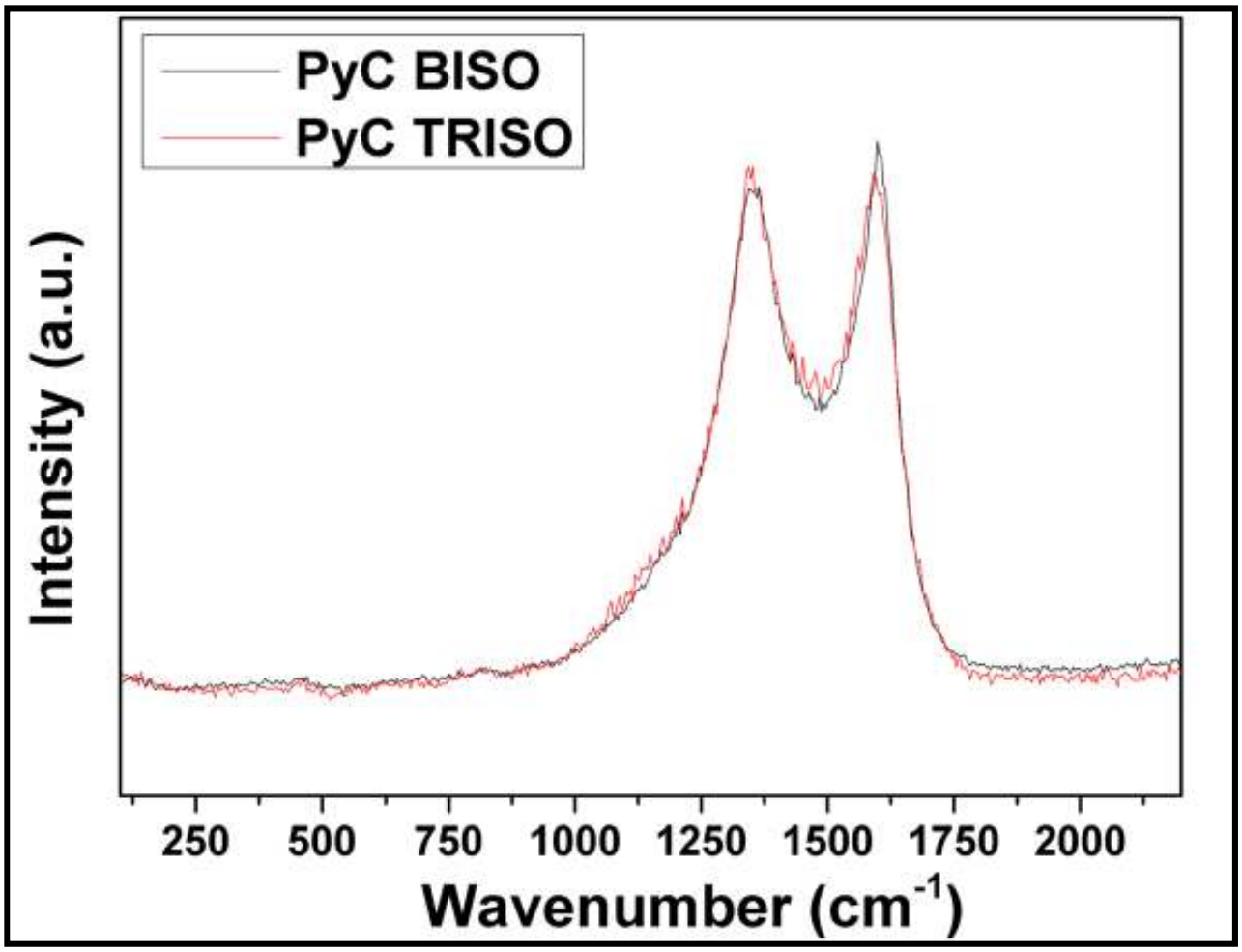

Fig. 4. *Raman spectra from 100 to 2300 cm^{-1} of external pyrolytic carbon in the BISO and TRISO particles.*

4.2. Solution analysis

The pH of the alteration solution is measured after each solution sampling during the corrosion. For the experiments conducted in reducing conditions (5% H_2/N_2), the results of pH measurements at 50°C and 90°C are plotted in Fig. 7 and Fig. 8, respectively. In all experiments we can notice that the solution pH, after an initial increase, remained stable at around 7.7 regardless the experimental conditions, e.g. temperature and number of particles. This indicates that even after 300 days of alteration at 50°C and 90°C the silicon carbide and pyrocarbon were highly stable.

The results of pH measurements for the experiments conducted under air are plotted in Fig. 9 and Fig. 10. We can notice that for the experiments conducted at 50°C the solution pH remained stable at around 7.7 – 7.8 regardless the number and nature of particles (BISO or TRISO) indicating the low alteration of SiC and pyrocarbon layers at 50°C under air. For the experiments conducted at 90°C, the pH values decreased from 7.6 - 7.7 to 7.2 - 7.3 after two months of alteration unlike in experiments conducted under reducing

conditions where the pH had no dependence on temperature. This may be explained by alteration of SiC and pyrocarbon layer at 90°C allowing formation of carbon oxide (CO and CO_2), carbonic acid ($CO_{2(aq)} + H_2O_{(l)} \rightarrow H_2CO_{3(aq)}$) and H_2SiO_3 acid as suggested in the literature [11-13]. However, the pH decrease under aerobic conditions can be beneficial for the stability and lifetime of SiC and Pyrocarbon layers because according to the literature the leaching rate of SiC and Pyrocarbon decreases in clay pore water with decreasing pH [8].

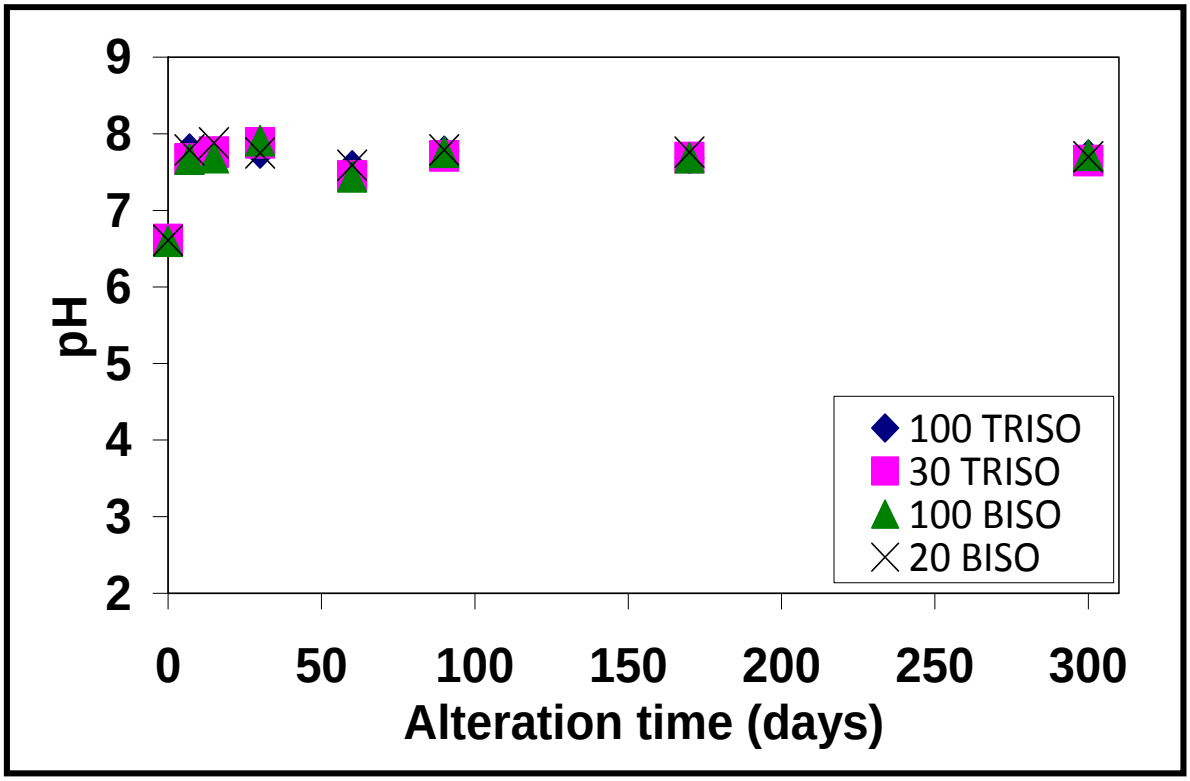

Fig. 7. *pH evolution with alteration time in experiment with BISO and TRISO particles and COX water at 50℃ under reducing conditions.*

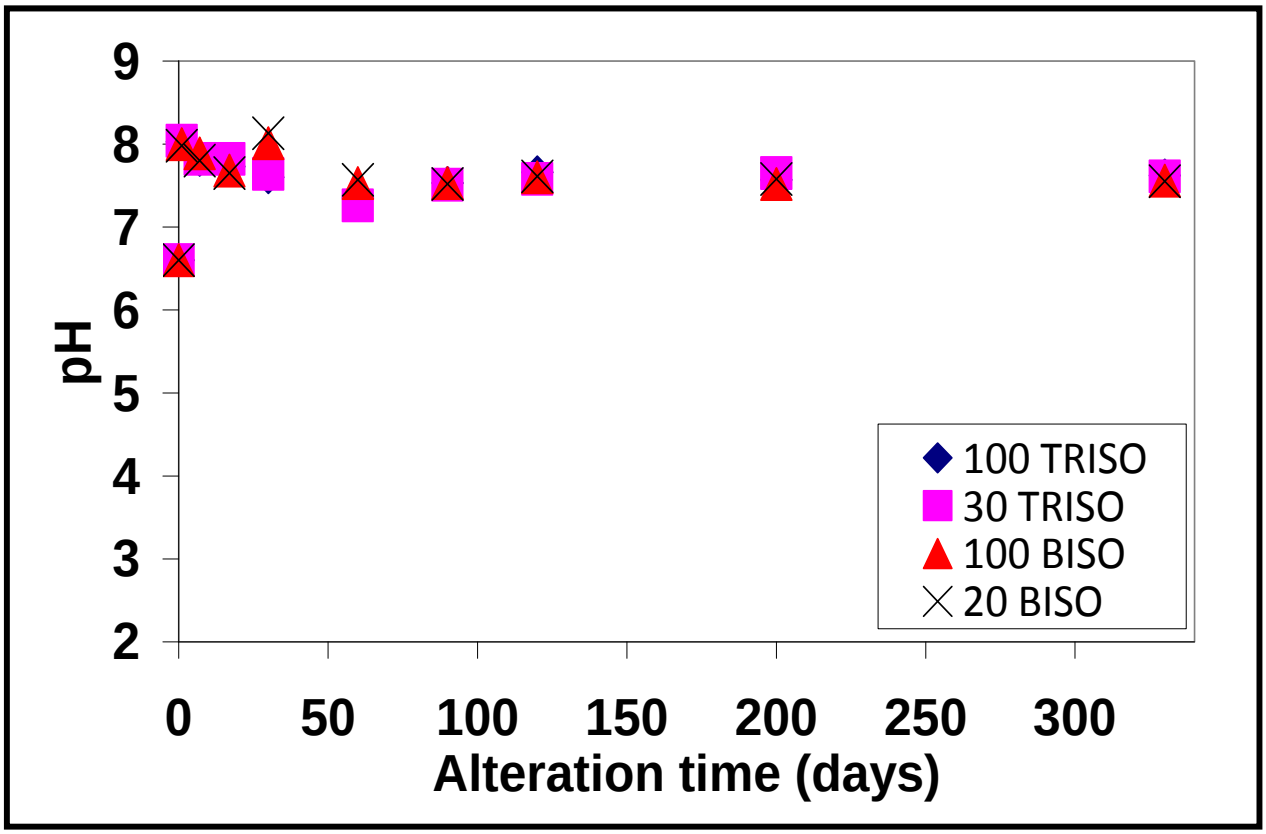

Fig. 8. *pH evolution with alteration time in experiment with BISO and TRISO particles and COX water at 90℃ under reducing conditions.*

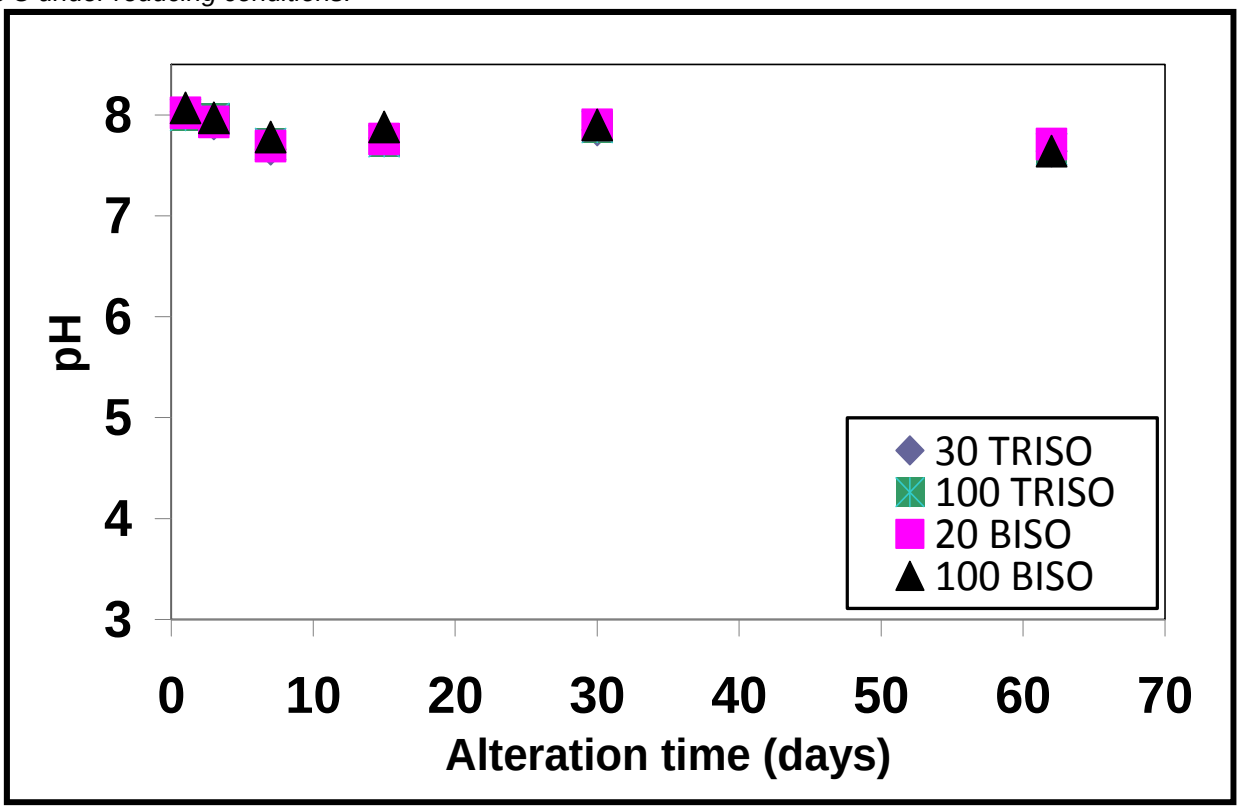

Fig. 9. *pH evolution with alteration time in experiment with BISO and TRISO particles and COX water at 50℃ under air.*

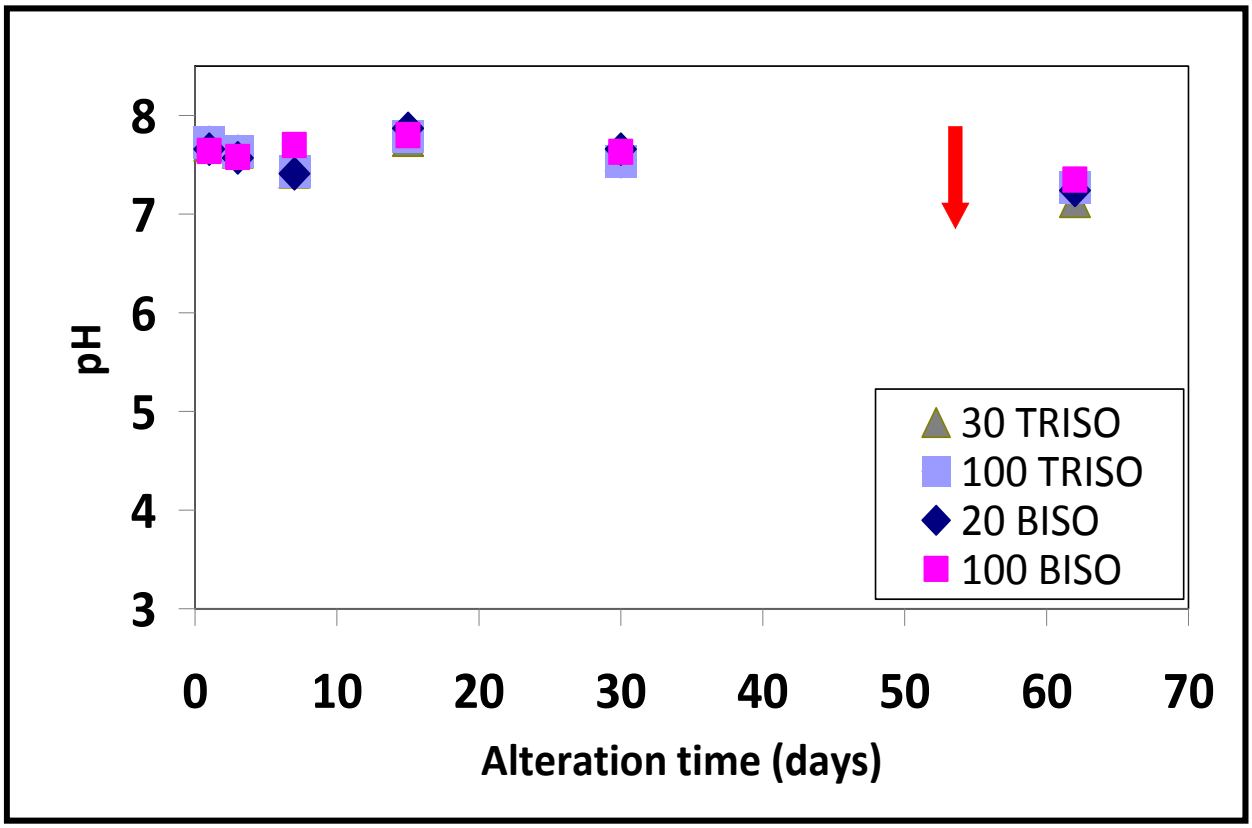

Fig. 10. *pH evolution with alteration time in experiment with BISO and TRISO particles and COX water at 90℃ under air.*

The silicon concentrations were measured by ICP-MS in the alteration solution of the TRISO particles. The results are plotted in Fig. 11 to 13. All analytical results were compared to blanks (COx water). For all experiments conducted under reducing conditions the silicon concentrations correspond to the initial concentration in COx water (Fig. 11 and 12), which confirms the high stability of SiC layer in the reducing conditions established in the autoclaves.

Under air (Fig. 13), at 50°C the silicon concentrations were stable and correspond to the initial concentration in COx water, while at 90°C, the Si-concentration decreases with the alteration time. This can be explained by the precipitation of silicon with magnesium of the COx water and formation of magnesium silicates. These analyzes confirm the results of pH measurements: stability of SiC and pyrocarbon layers and low alteration under reducing conditions and confirm an eventual oxidation at 90°C under air.

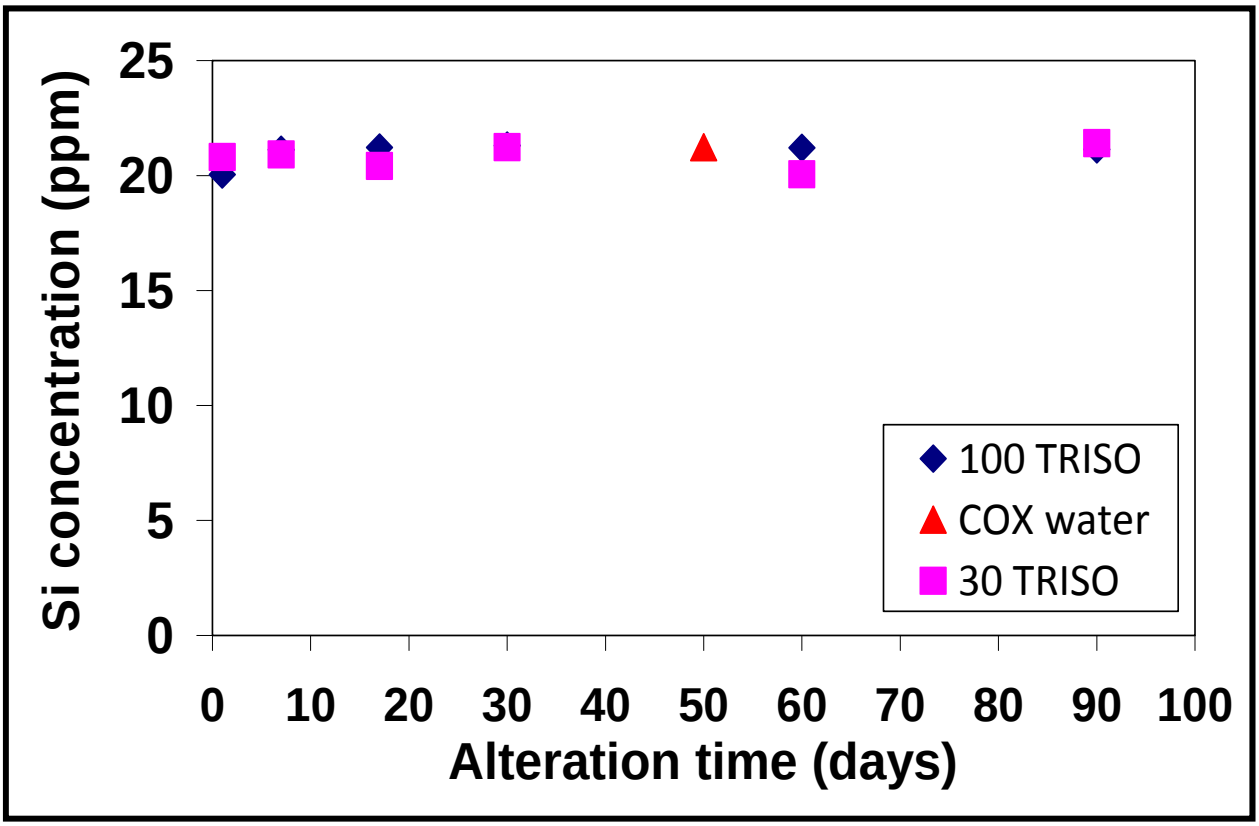

Fig. 11. *Evolution of Si concentration with alteration time in experiment with TRISO particles and COX water at 90℃ under reducing conditions.*

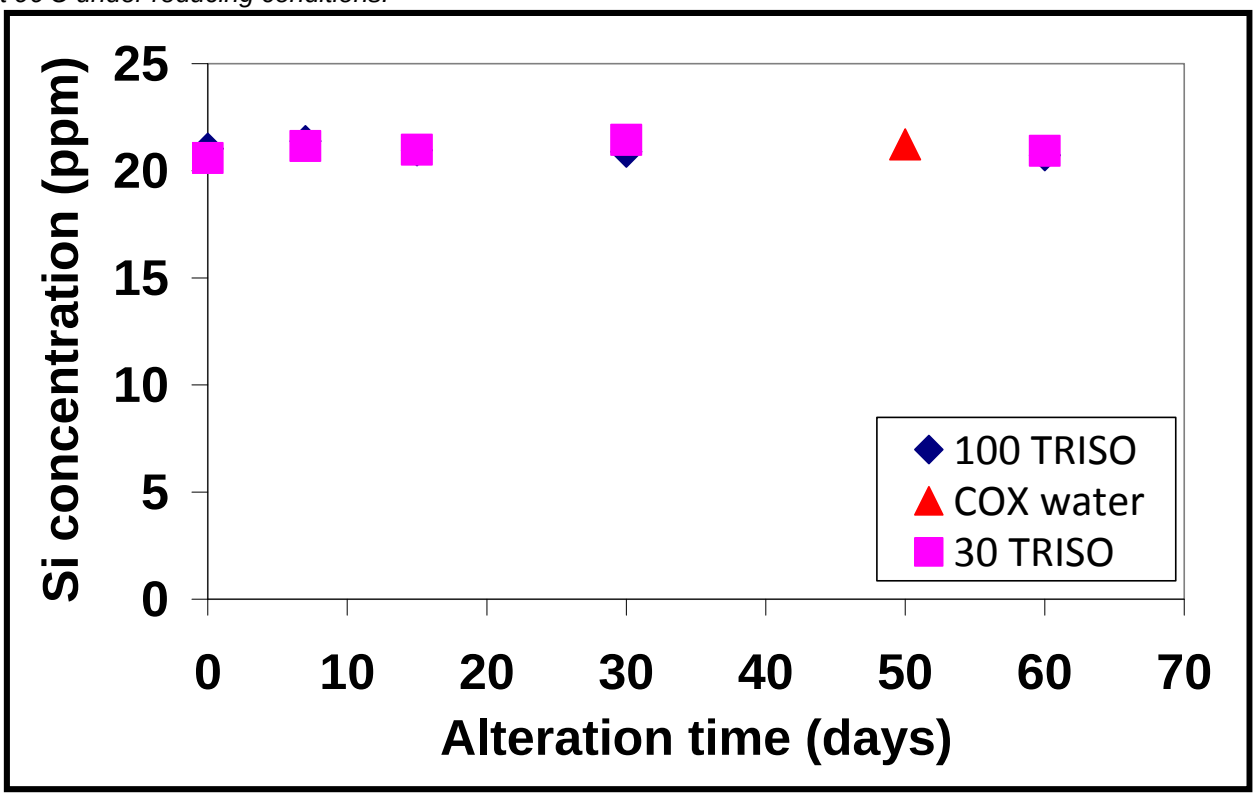

Fig. 12. *Evolution of Si concentration with alteration time in experiment with TRISO particles and COX water at 50℃ under reducing conditions.*

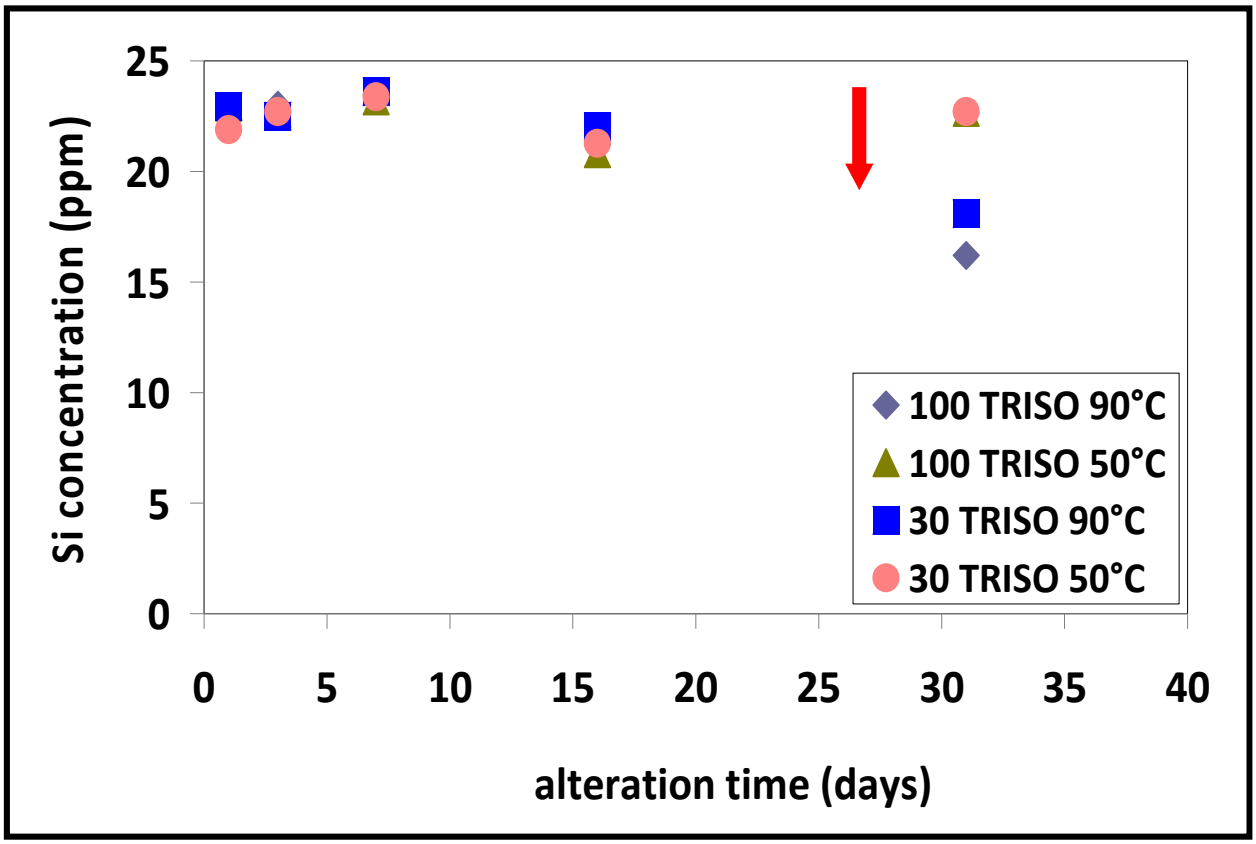

Fig. 13. *Evolution of Si concentration with alteration time in experiment with TRISO particles and COX water at 50 and 90℃ under air.*

To detect a possible precipitation of Ca, and Mg, we performed analyses of these elements by ion-chromatography. Fig. 14 to Fig. 16 shows the evolution of the concentration of magnesium and calcium with the alteration time at 50°C and 90°C. Under H_2 atmosphere, we can conclude that concentrations of these elements remained within the bar error after few months of alteration. The same trend was observed under air.

The Mg and Ca concentrations were stable (within the bar error) under air. However, this does not exclude the reaction of a small fraction of these elements with particles, in particular SiC.

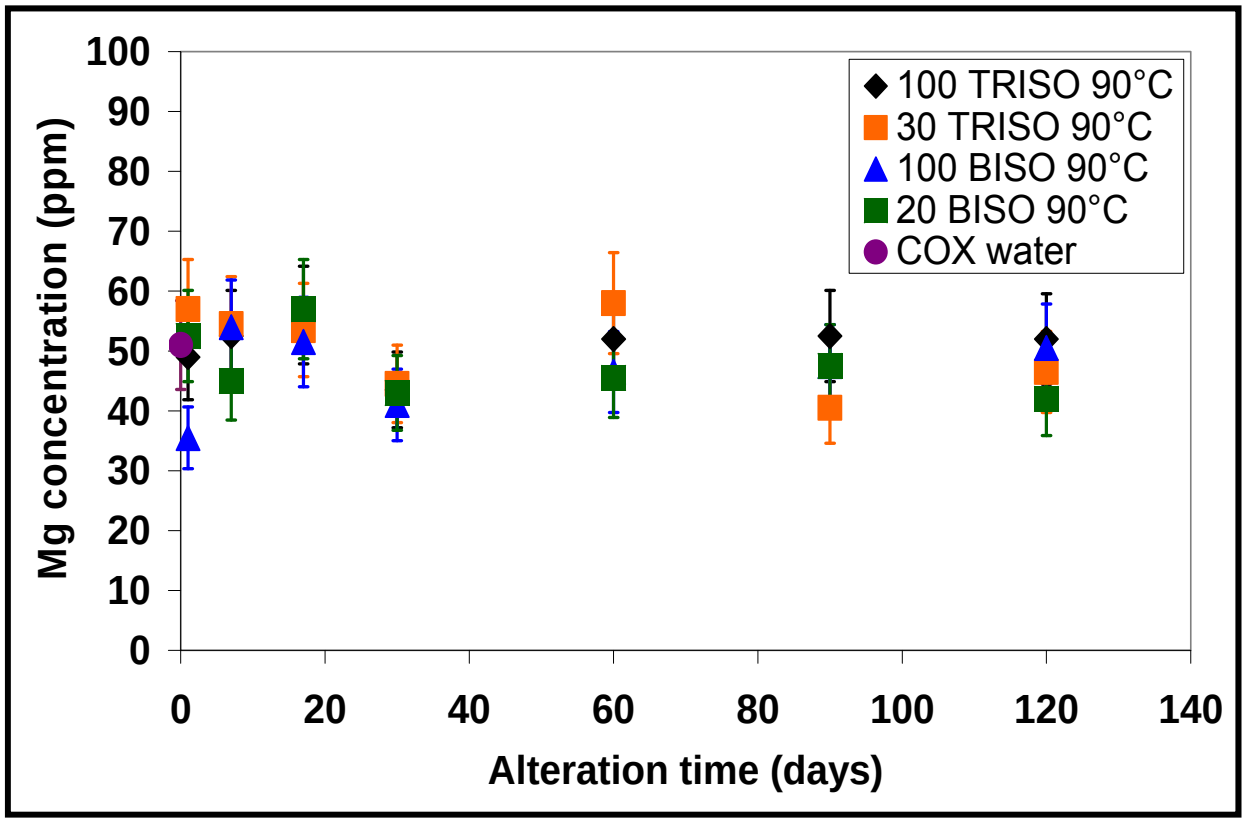

Fig. 14. *Evolution of the magnesium concentration at 90℃ under reducing conditions.*

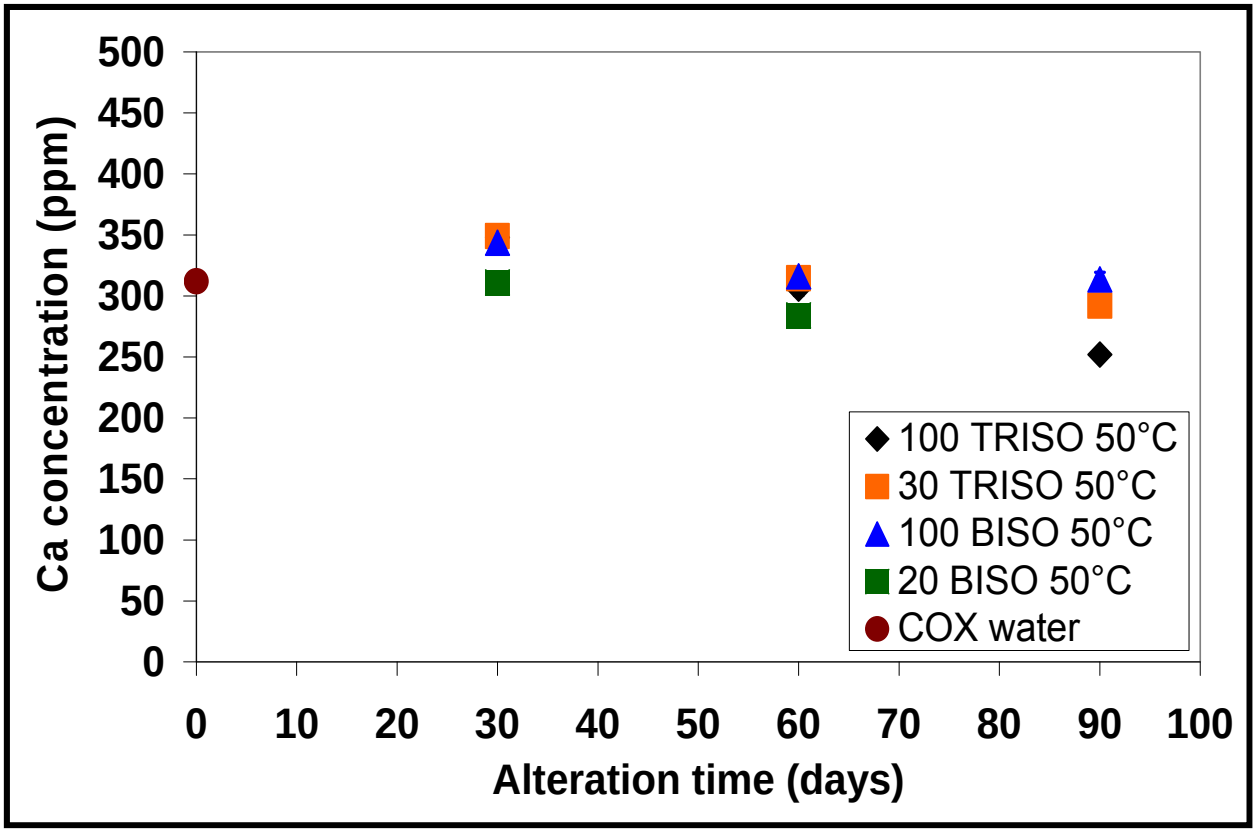

Fig. 15. *Evolution of the calcium concentration at 50℃ under reducing conditions.*

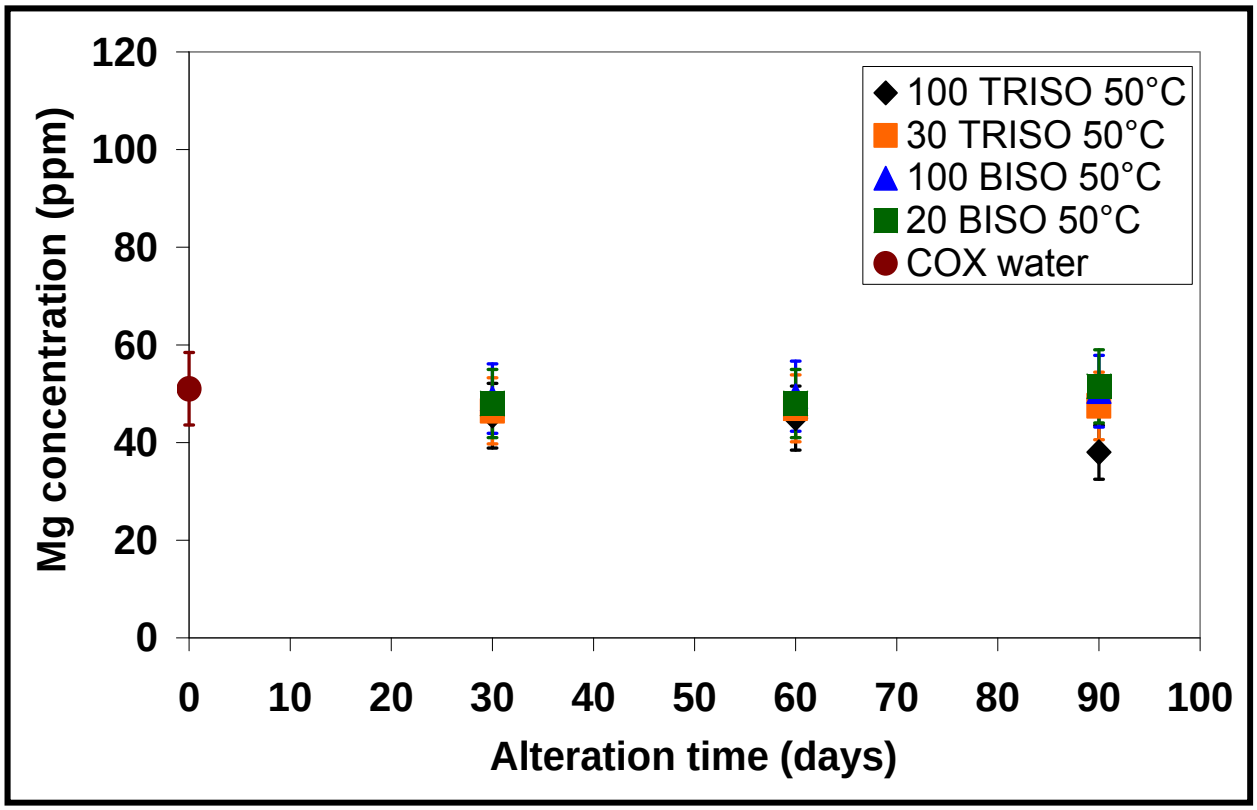

Fig. 16. *Evolution of the magnesium concentration at 50℃ under reducing conditions.*

4.3. Solid analysis

4.3.1. SEM, EDX and EPMA analyses

Particles of each system were removed and dried for SEM characterization, EDX, EPMA, μ-Raman and XPS analysis in order to study the degree of alteration of SiC layer in the TRISO particles and the carbon layer of BISO particles. No difference was found from SEM/EDX between 100 and 30 TRISO system and between 100 and 20 BISO systems. An example of the TRISO particles micrographs after 230 days of alteration under reducing conditions at 90°C is given in Fig. 17 and Fig. 18. EDX analyzes are summarized in the Table 5. We detect only low amount of oxygen and elements initially present in COx water (Na, Cl, Si, Mg, Ca...). Only traces of oxygen were detected indicating the high chemical durability of SiC and PyC layers in the absence of oxygen. The amount of oxygen is compared to that measured in the pristine TRISO and BISO particles; oxygen is relatively low under reducing conditions (H_2/N_2), while under air, the amount of oxygen is very important, indicating that the alteration of PyC and SiC were found to be higher under air as compared to H_2/N_2 atmosphere. The oxygen analyzes are further confirmed by EPMA, which is more quantitative than EDX.

Example of micrograph of TRISO particles altered under aerobic conditions is given in Fig. 19 and Fig. 20. One can see a clear alteration of the SiC layer and the formation of fibrous material enriched in Si and Mg, likely corresponding to clay mineral such as sepiolite ($Mg_4Si_6O_{15}(OH)_2$, $6H_2O$) [17] as indicated by the EDX spectrum in Fig. 19. Geochemical calculations using the PHREEQC V1.02 code [18] showed that the COx water is under-saturated with respect sepiolite suggesting a local super-saturation with respect this mineral at the interface solution/SiC. This is supported by the work of Fenter and Sturchio [19] and Kerisit and Liu [20] who suggested that solid/water interaction is driven by dissolution in an ultrathin interfacial fluid film (< 3 nm) leading to local super-saturation. Table 5 clearly shows a surface enrichment in oxygen which caused both SiC and pyrolytic carbon oxidation under aerobic conditions at 90°C.

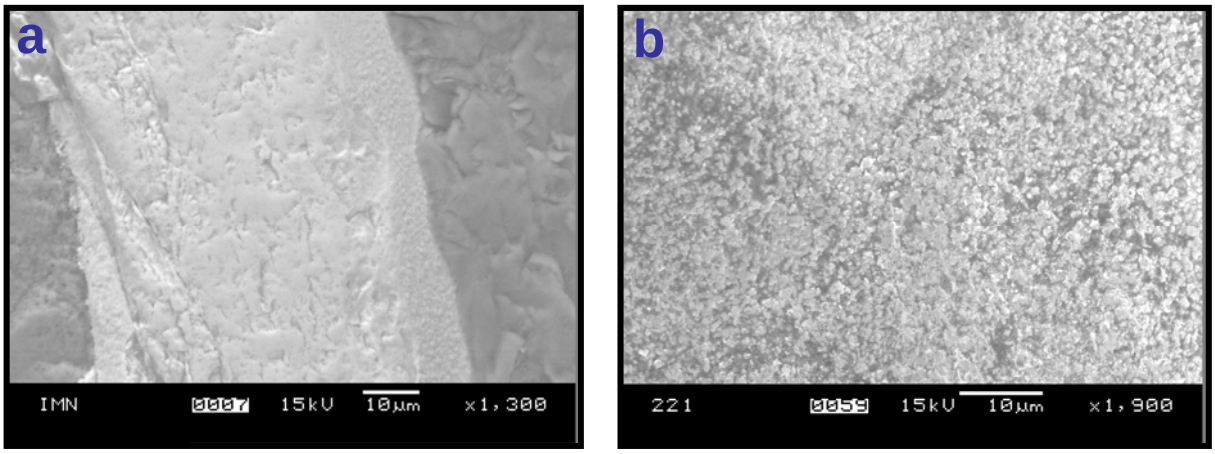

Fig. 17. *SEM micrographs of a TRISO particle (100 TRISO system) showing external SiC layer after 230 days of alteration at 90℃ in COX water under reducing condi tions, (a): cross section, (b): surface of altered particle.*

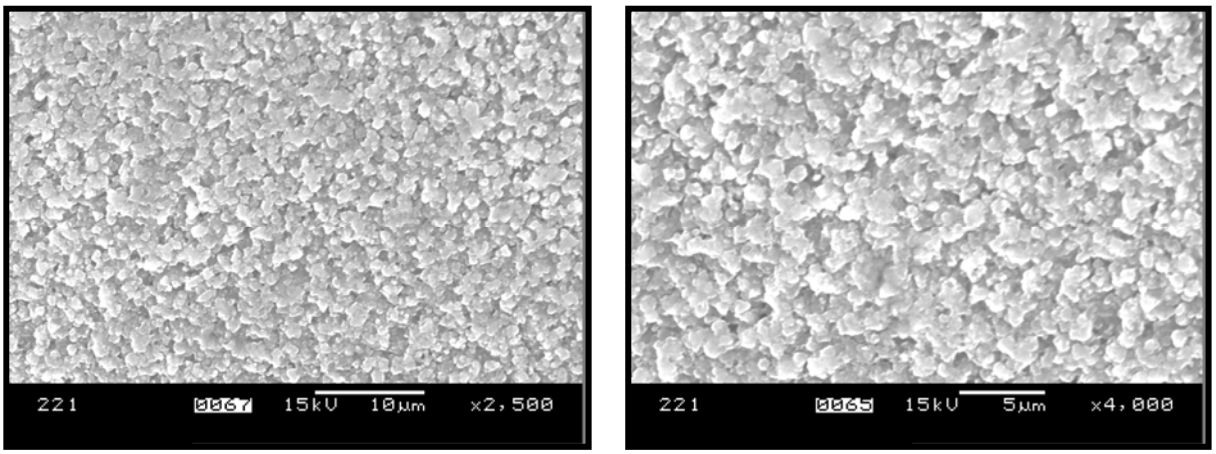

Fig. 18. *SEM micrographs of a BISO particle (100 BISO system) showing the external PyC layer after 230 days of alteration at 90℃ in COX water under reducing conditions.*

Table 5
EDX analysis of TRISO and BISO particles altered at 90℃ under air and reducing conditions (5% H_2/N_2) after 90 days of alteration.

	Under 5% H_2/N_2			Under air		
System	at. % Si	at. % C	at. % O	at. % Si	at. % C	at. % O
100 TRISO	49.6	48.4	1.1	36.4	32.0	31.7
30 TRISO	48.6	47.2	4.2	36.8	28.2	32.8
100 BISO		97.3	2.7	-	49.0	39.7
20 BISO		96.9	3.2	-	68.0	27.3
Pristine particles						
	at. % Si		at. % C		at. % O	
Pristine TRISO	49.8		49.0		2.1	
Pristine BISO	0		98.0		2.0	

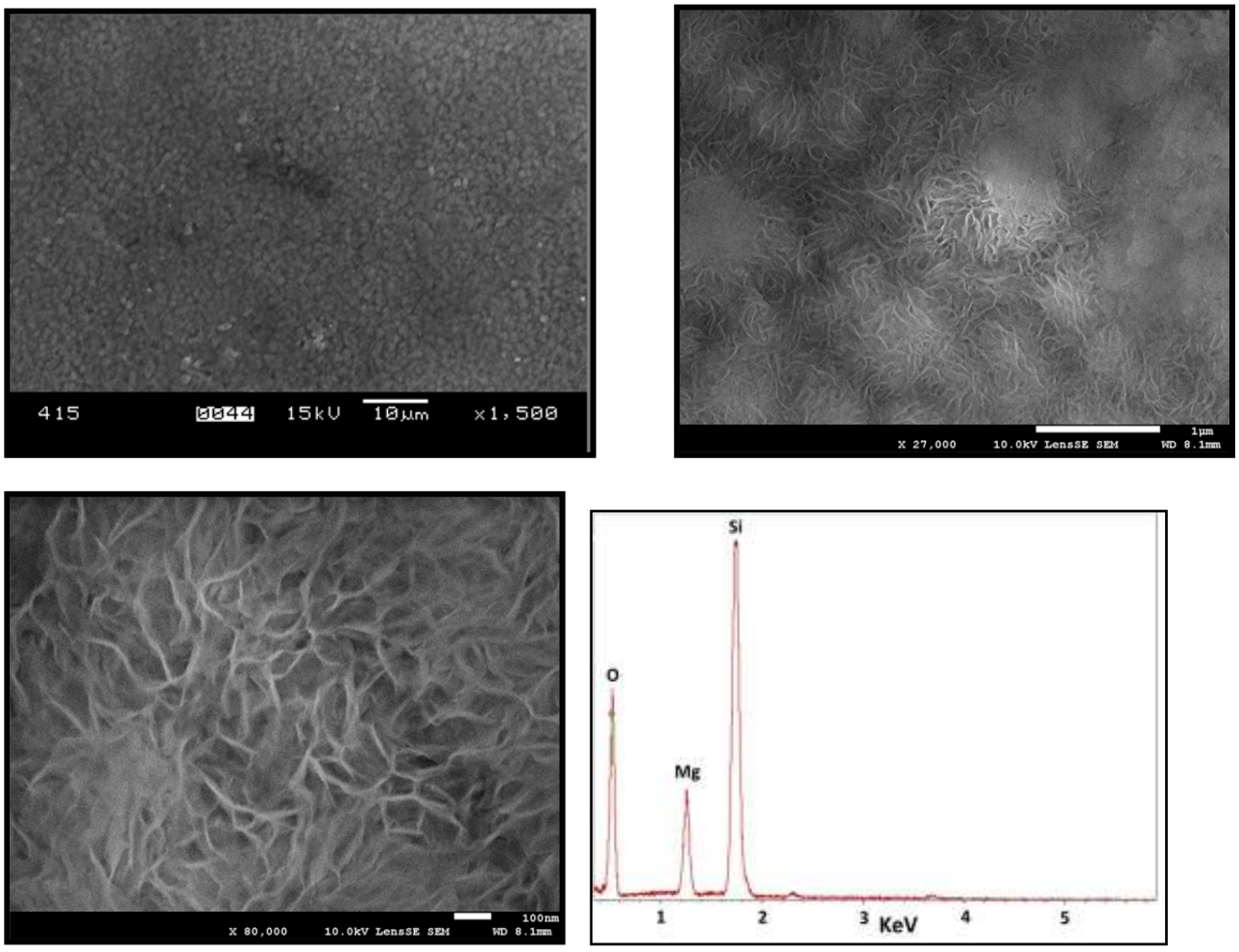

Fig. 19. *SEM micrographs and corresponding EDX spectra of a TRISO particle (100 TRISO system) showing external SiC layer after 90 days of alteration at 90℃ in COX water under aerobic conditions showing the* formation of clay-type phases with composition close to that of sepiolite.

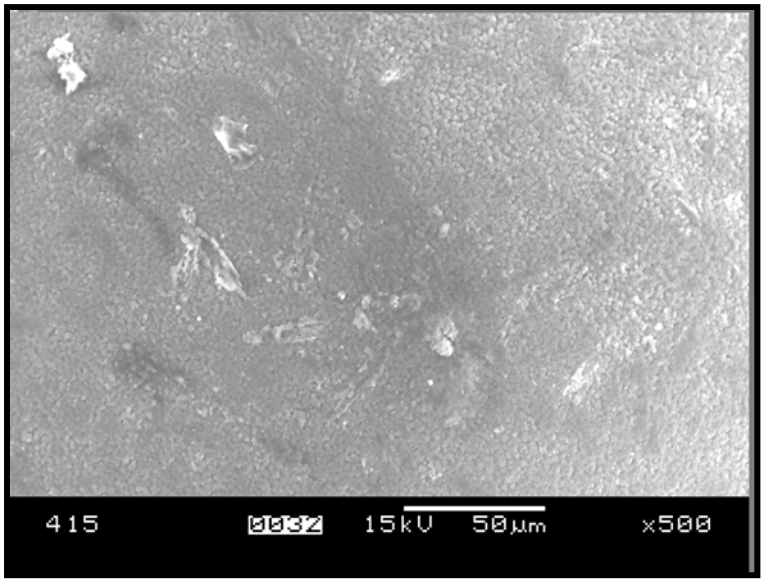

Fig. 20. *SEM micrographs of BISO particles (100 BISO system) altered at 90℃ in COX water for 90 days under aerobic conditions showing external carbon with salt-like phases precipitated from water.*

At 50°C, the micrographs of both TRISO and BISO particles altered for 230 days under reducing conditions show no sign of alteration (Fig. 21 and Fig. 22). The results are similar for experiments under aerobic conditions (Fig. 23 and Fig. 24). The chemical analyses of the particles altered at 50°C under reducing and aerobic conditions are given in Table 6. We notice a slight oxidation of the particles at 50°C under oxidizing conditions.

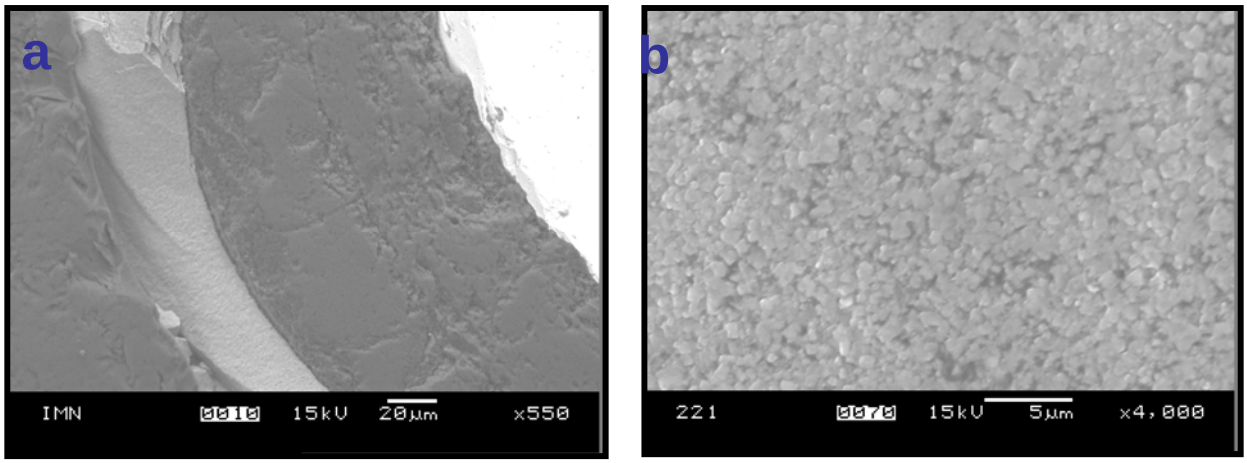

Fig. 21. *SEM micrographs of a TRISO particle (100 TRISO system) showing external SiC layer after 230 days of alteration at 50℃ in COX water under reducing condi tions, (a): cross section, (b): surface of altered particle.*

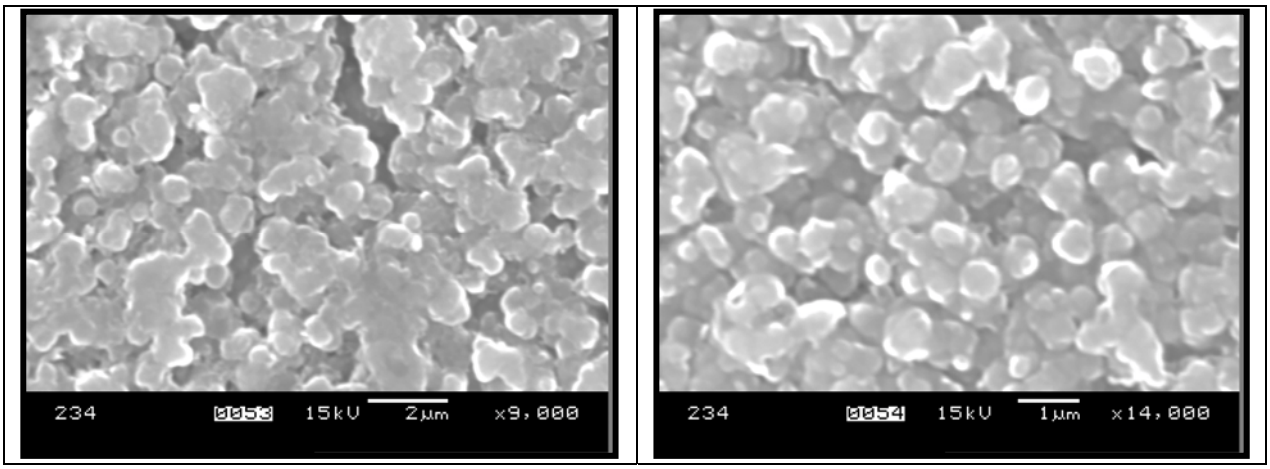

Fig. 22. *SEM micrographs of a BISO particle (100 BISO system) showing external the external carbon layer after 230 days of alteration at 50℃ in COX water under reducing conditions.*

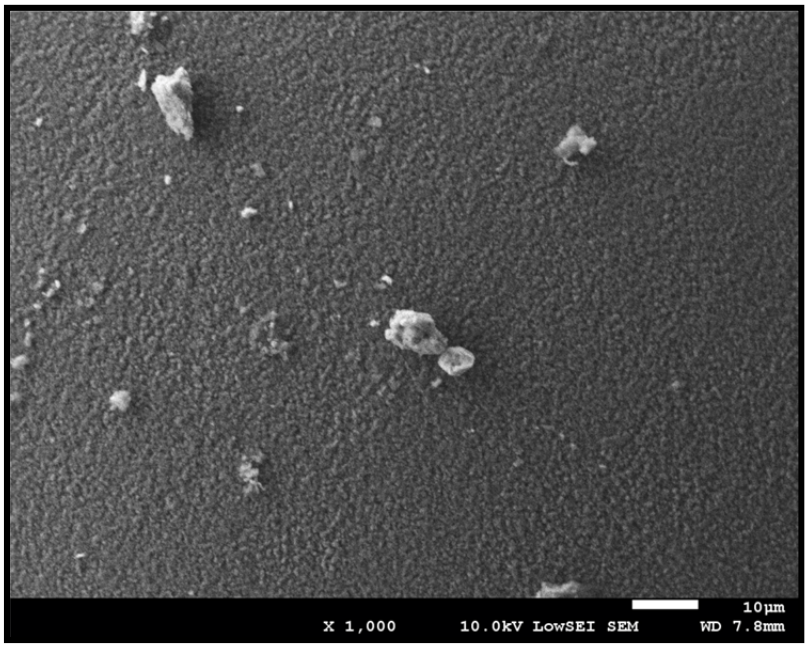

Fig. 23. *SEM micrographs of a TRISO particle (100 TRISO system) showing external SiC layer after 90 days of alteration at 50℃ in COX water under aerobic conditions.*

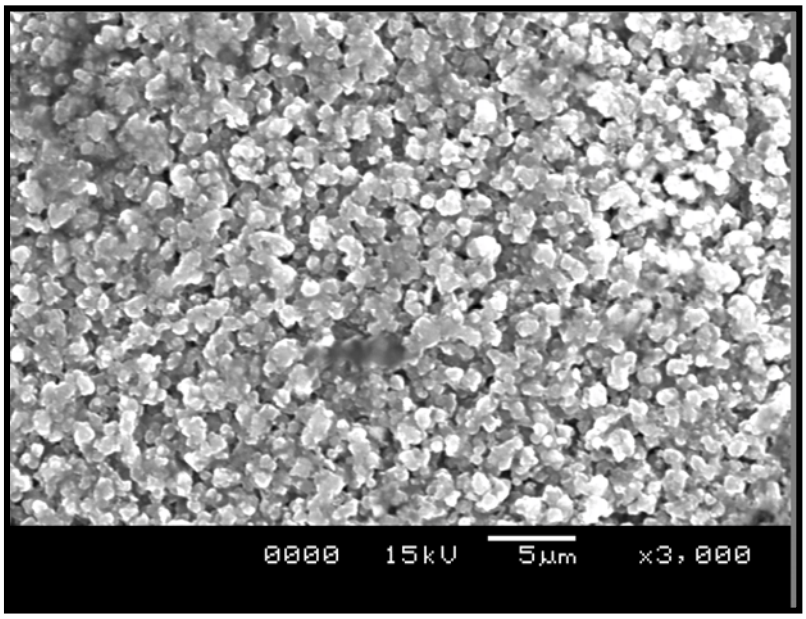

Fig. 24. *SEM micrographs of a BISO particle (100 BISO system) showing external the external carbon layer after 90 days of alteration at 50℃ in COX water under aerobic conditions.*

Table 6

EDX analysis of TRISO and BISO particles at 50℃ under air and reducing conditions (5% H2/N2) after 3 months of alteration.

	Under 5% H_2/N_2			Under air		
System	at. % Si	at. % C	at. % O	at. % Si	at. % C	at. % O
100 TRISO	47.6	50.8	1.6	38.7	58.6	2.5
30 TRISO	47.4	50.5	2.1	44.5	53.5	2.1
100 BISO	-	99.1	0.8	-	96.2	3.5
20 BISO	-	98.7	1.0	-	96.5	3.1

The oxygen measurements have been performed by EPMA for experiments at 90°C. The results are in good agreement with EDX analysis (Table 7). As we can see, only 7 to 8 atomic % of oxygen were detected after one year of alteration under reducing conditions, while under air the amount of oxygen is important (34 to 35 atomic %) after only 90 days of alteration. The pyrolytic carbon of BISO particles is not oxidized under H_2/N_2 even after 1 year of alteration.

Table 7
EPMA analysis of TRISO and BISO particles at 90℃ under air and reducing conditions (5% H_2/N_2).

System	at. % Si	at. % C	at. % O
Pristine TRISO	48.5	49.7	1.8
Pristine BISO	0	99.1	0.9
100 TRISO altered at 90°C 1 year under H_2/N_2	46.7	45.9	7.4
30 TRISO altered at 90°C 1 year under H_2/N_2	46.1	42.0	7.9
100 BISO altered at 90°C 1 year under H_2/N_2	0	99.0	1.0
20 BISO altered at 90°C 1 year under H_2/N_2	0	98.8	1.2
100 TRISO altered at 90°C 3 month under air	42.1	23.9	34.0
100 BISO altered at 90°C 3 month under air	1.7	63.3	35.6

4.3.2. Micro-Raman spectroscopy analysis

Micro-Raman analyses were performed in order to detect a possible oxidation of SiC and pyrocarbon with the possible formation of SiO_2 and C=O bands or other alteration products. Raman spectra of pristine and altered SiC layer in TRISO particles under aerobic and reducing conditions at 90°C and 50°C are shown in Fig. 25 and Fig. 26. The characteristic Raman lines of cubic silicon carbide, which occur at 795 cm^{-1} (transverse optical mode) and ~970 cm^{-1} (longitudinal optical mode) [21] are observed. The Raman spectrum of graphite usually shows two modes, zone center E_{2g} phonon mode at around 1580-1600 cm^{-1} (commonly known as G-peak, sp^2 mode) and K-point phonons at around 1350 cm^{-1} (commonly known as D-peak: disordered allowed zone edge mode of graphite). The D band is observed in amorphous or nanocrystalline graphitic carbon, and it is usually related to the disorder associated with the finite crystallite size [22-24].

No differences are detected between pristine and altered particles by Raman spectroscopy. The small band detected near 1715 cm^{-1} correspond to the stretching of carbonyl group (C=O), present both in pristine and altered particles at 50°C and 90°C probably due to the surface oxidation of SiC. This indicates that the analyzed thickness (~1 µm) is mostly made of original SiC.

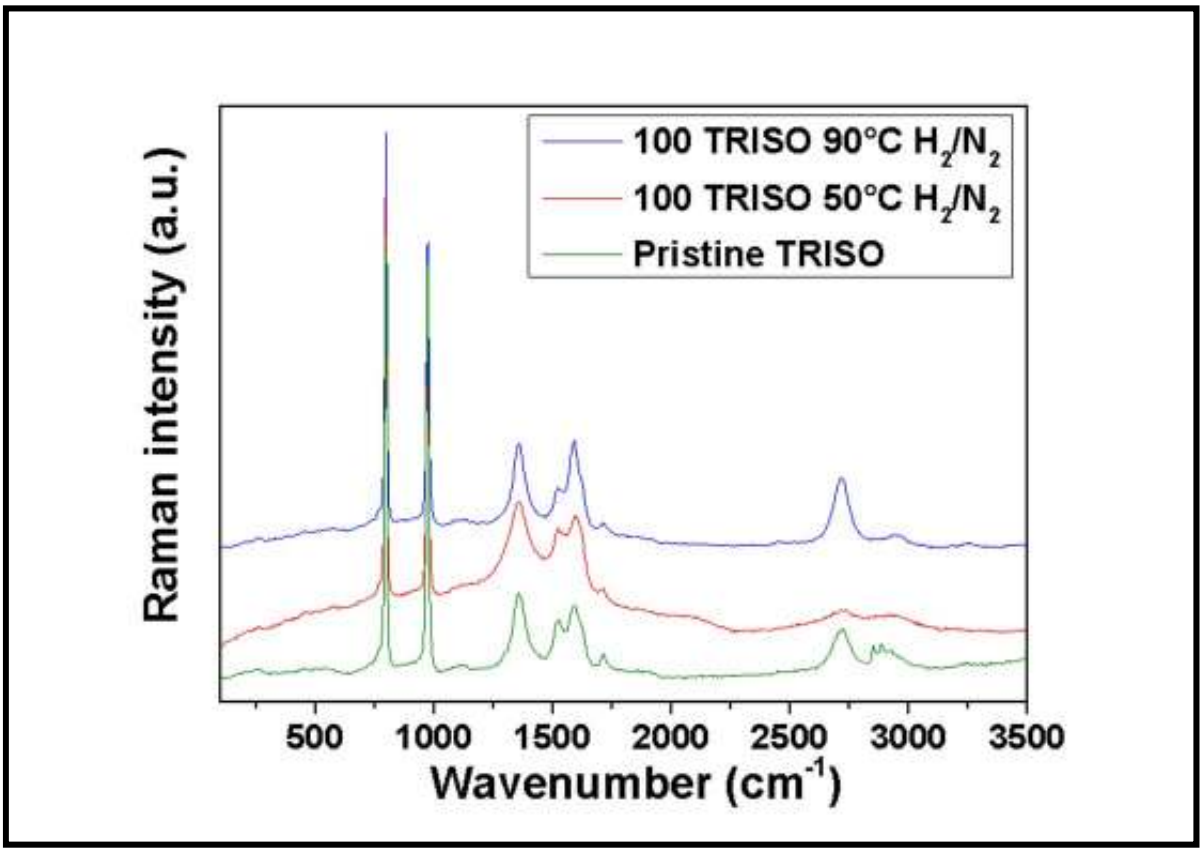

Fig. 25. *Raman Spectra of SiC layer in the 100 TRISO system after 3 months of alteration in COX water at 50℃ and 90℃ under reducing conditions compared to pristine TRISO spectrum.*

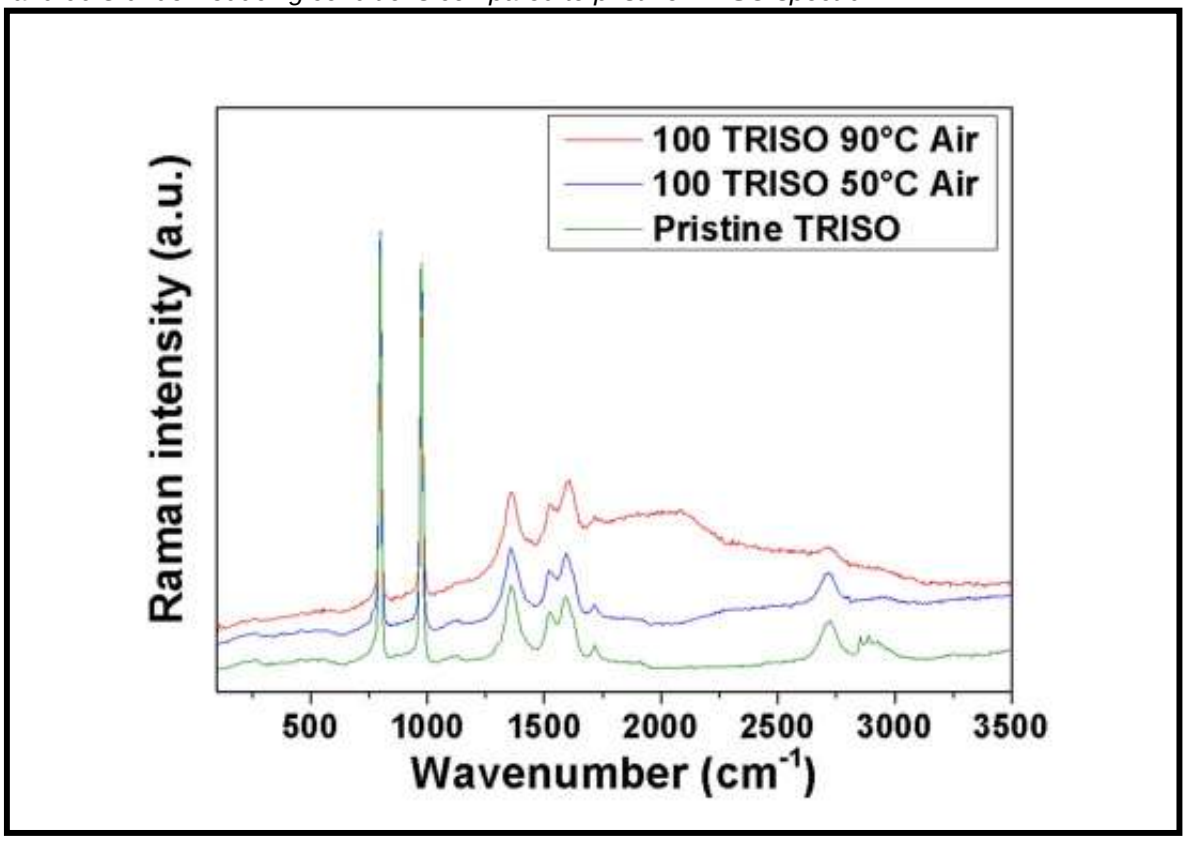

Fig. 26. *Raman Spectra of SiC layer in the 100 TRISO system after 3 months of alteration in COX water under aerobic conditions.*

4.3.3. X-ray photoelectron spectroscopy

The X-ray photoelectron spectra of TRISO particles are shown in Fig. 27. The O_{2s} and O_{1s} photoelectron lines are located near 23.1 and 531 eV, respectively. The Si_{2p} and Si_{2s} photoelectron line at 102 eV and 152 eV, respectively. C_{1s} peak at around 285 eV. Mg_{2p} and Mg_{2s} photoelectron lines are located at 48.5 eV and 87.5 eV, respectively (Fig. 27). The O_{1s}, Si_{2p}, C_{1s} and Mg_{2p} XP spectra for pristine and altered TRISO particles are shown in Fig. 28 to Fig. 31.

The O_{2s} and O_{1s} atomic orbital lines are observed at 23.1 eV and 530.5, respectively. Fig. 28 shows the O_{1s} X-ray photoelectron band. The intensity of this band is higher for the particles altered under air and increases with temperature. The peak at 530.5 eV corresponds to O_{1s} in the SiO_2 (Fig. 28). We can also see the shift of the photoelectron line from 529 eV in the pristine TRISO to 530.5 eV in the particles altered under air at 90°C. The intensity of this peak increases under air and the increasing is pronounced in the experiment conducted at 90°C under air indicating a higher alteration of SiC under air compared to H_2/N_2 atmosphere. This is confirmed in the O_{2s} photoelectron line near 23.1 eV. It is reported in the literature that this binding energy shift may result from (valence) electron density being drawn away from others atoms (carbon) to oxygen and Si tetrahedra (via Si–O covalent bonds) and the result of increasing of the quantities of SiO_2 at the surface of the material [25]. This is manifested by the shift of the binding energies of O_{1s} peaks systematically to higher binding energy with increased SiO_2 content. The peak near 531 eV is attributed to the O_{1s} emission from silicon oxides and the binding energy shifts correspond to the status of silicon atoms oxidation [26].

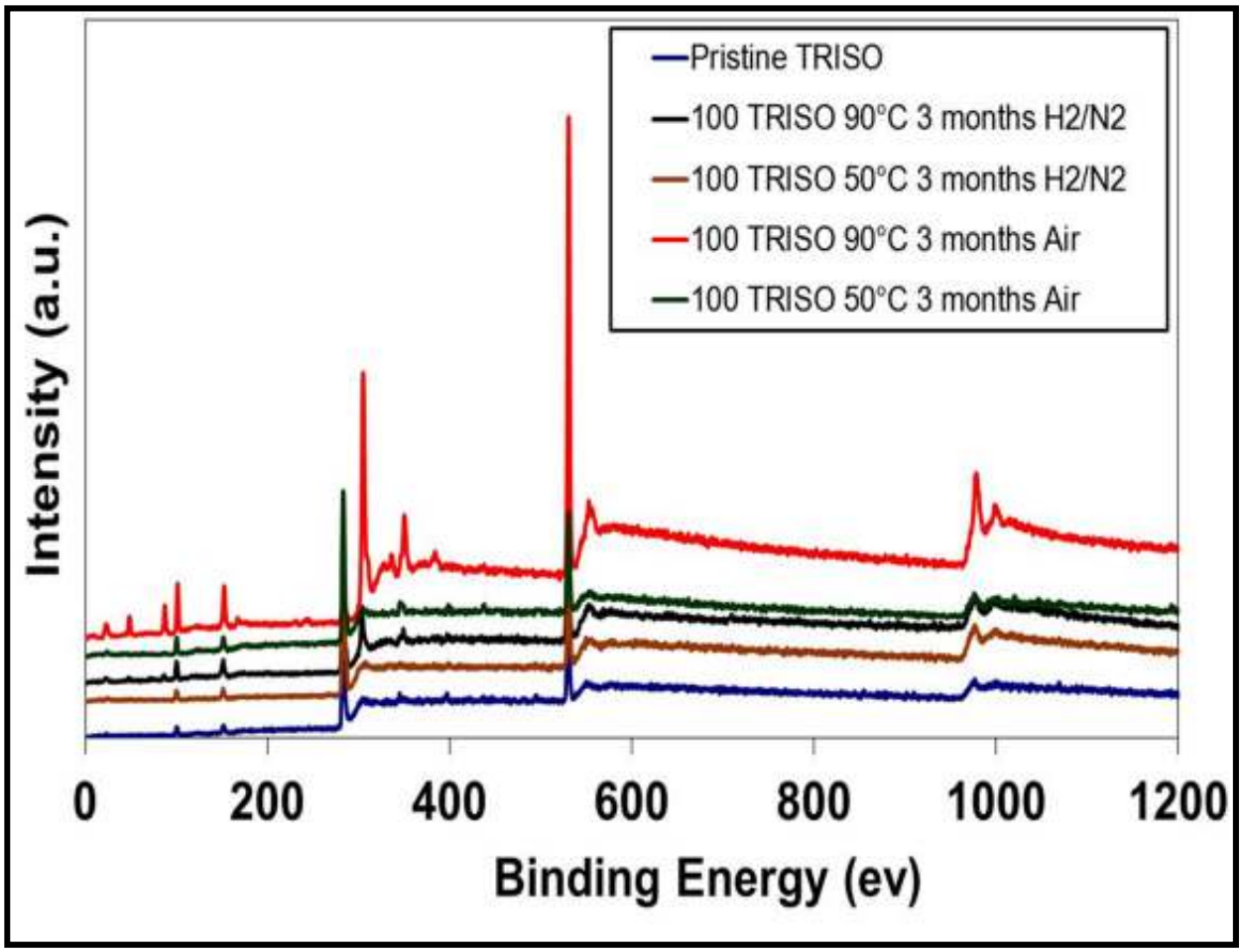

Fig. 27. *X-ray photoelectron spectra of TRISO particles before and after 3 months of alteration at 50℃ and 90℃ under air and under reducing conditions.*

Under oxic atmosphere the Si_{2p} peak shifts to a higher binding energy from 100.5 to 101.5 eV (Fig. 29), which is consistent with the formation of silica (SiO_2) [27]. This peak increases under air and the increasing is pronounced in the experiment conducted at 90°C under air. The same trend is observed for the Si_{2s} peak.

For C_{1s} spectra (Fig. 30), the peaks at around 284 eV correspond to sp2 carbon atoms [28]. The presence of lower energy peak at around 283 eV corresponds to carbon atoms bonded to silicon (carbon peak of silicon carbide) [30]. The feature at 286.6 eV is assigned to CO contamination formed on the particles surface present in both pristine and altered particles [27, 30]. The peak at 283 eV (C-Si band in SiC) decreases for the particles altered at 90°C (Fig. 30). The decrease is more important in the experiments conducted under air at 90°C indicating the oxidation of SiC layer and the formation of silica, the carbon is probably leached in the solution.

The Mg_{2s} and Mg_{2p} binding energy is relatively invariant with chemical state, so chemical nature of magnesium on the particle surface can be difficult to detect by XPS. However, as we can see in Fig. 31, there is an increase of the magnesium signal at 90°C under air (Mg_{2s} band) compared with experiment

conducted under reducing conditions (Fig. 31). The same trend is observed for the Mg_{2p} band. This confirms the SEM/EDX analyses and the formation under oxic conditions of magnesium silicates like sepiolite at the surface of the TRISO particles.

The shifts toward higher energies observed for oxygen and silicon peaks and the decrease of C_{1s} peak intensity for the experiments conducted under air suggest a clear alteration of SiC. From the energies of these elements the bond type can be deduced and suggest the formation of SiO_2.

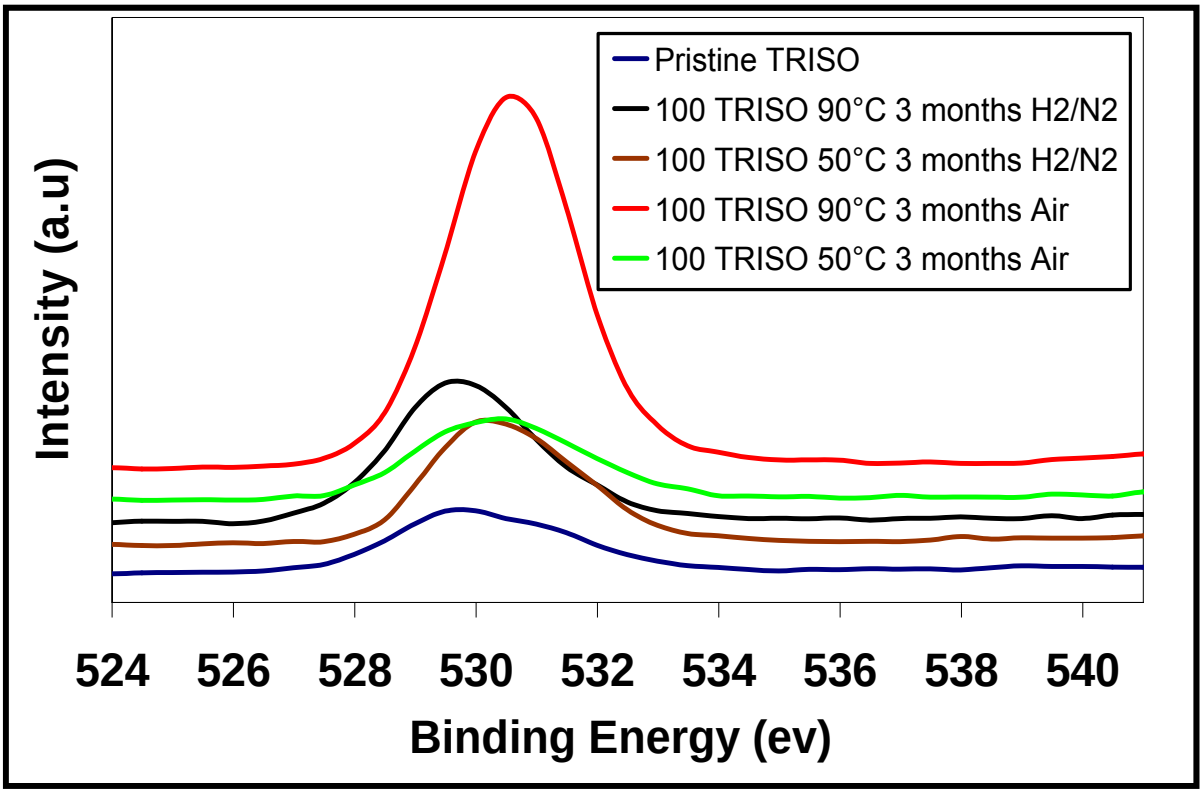

Fig. 28. *O_{1s} XPS spectra of TRISO particles before and after* 3 months of *alteration at 50℃ and 90℃ under air and under reducing conditions.*

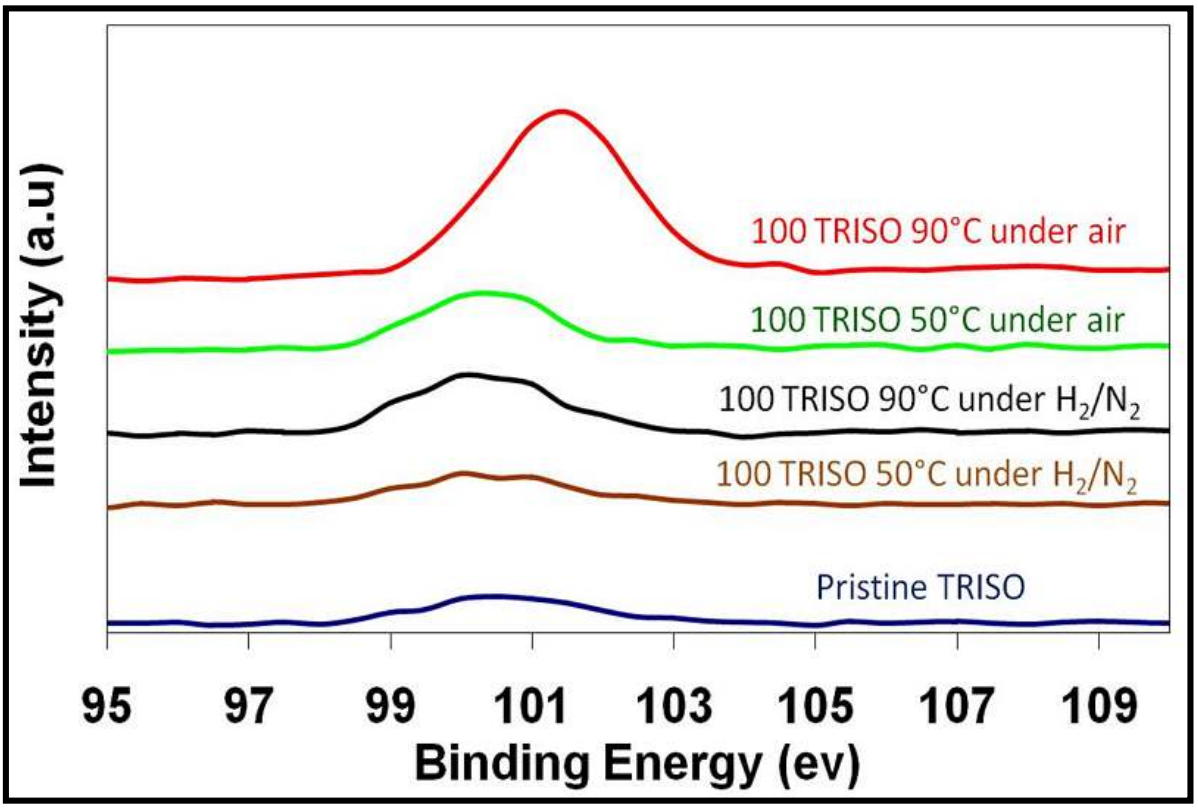

Fig. 29. *Si_{2p} XPS spectra of TRISO particles before and after* 3 months *of alteration at 50℃ and 90℃ under air and under reducing conditions.*

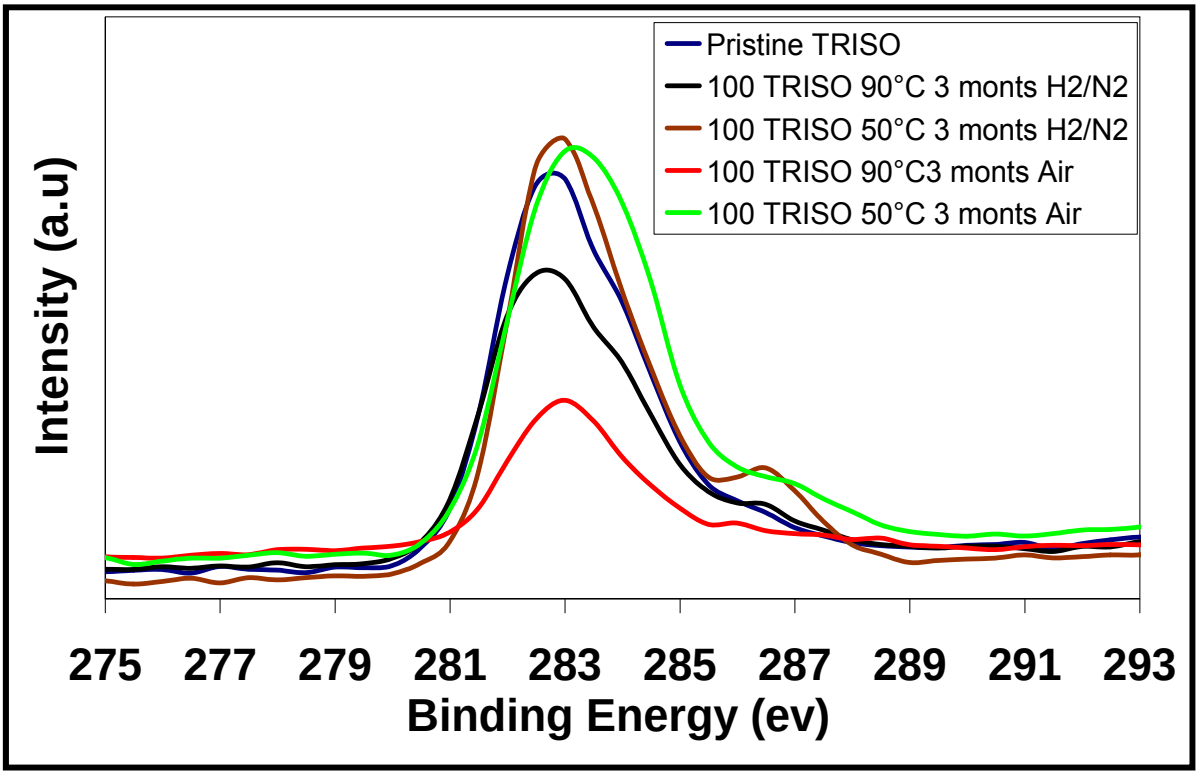

Fig. 30. *C_{1s} XPS spectra of TRISO particles before and after* 3 months of *alteration at 50℃ and 90℃ under air and under reducing conditions.*

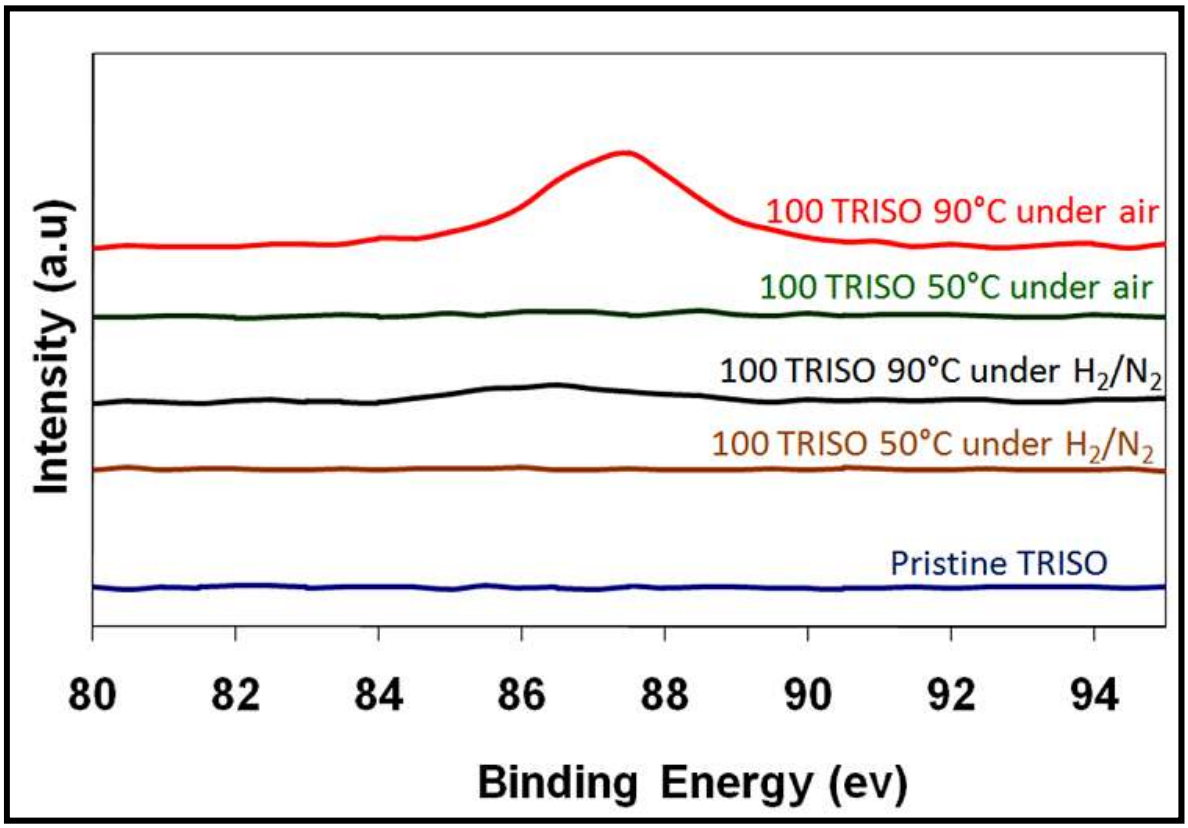

Fig. 31. *Mg_{2s} XPS spectra of TRISO particles before and after* 3 months of *alteration at 50℃ and 90℃ under air and under reducing conditions.*

Pristine and altered BISO particles were also analysed by XPS. The XPS spectra of oxygen and carbon show the same behaviour as the TRISO particles, meaning a small increase of oxygen band under reducing conditions and high increase under air. For the C_{1s} band, we can see in Fig. 32 the decrease of the sp_2 carbon atoms band at 284.5 eV (C-C) in the altered particles and the decrease is more pronounced under air. We have not been able to explain the shift to lower energies observed in the altered particles (from 284.5 to 282.7 eV). In the literature the bands between 282 eV and 283 eV correspond to C-Si, C-Ti, C-B... No significant differences are observed in the C-O (286.5 eV) and C=O (287.8 eV) band between the particles altered under air and under reducing conditions. In the literature, the deconvolution of the main peak in the C_{1s} region is generally more difficult and ambiguous, as the relative contribution to the peaks from oxygenated groups compared to that from the asymmetrically shaped graphitized carbon signal is too small to be isolated directly from the spectra [31].

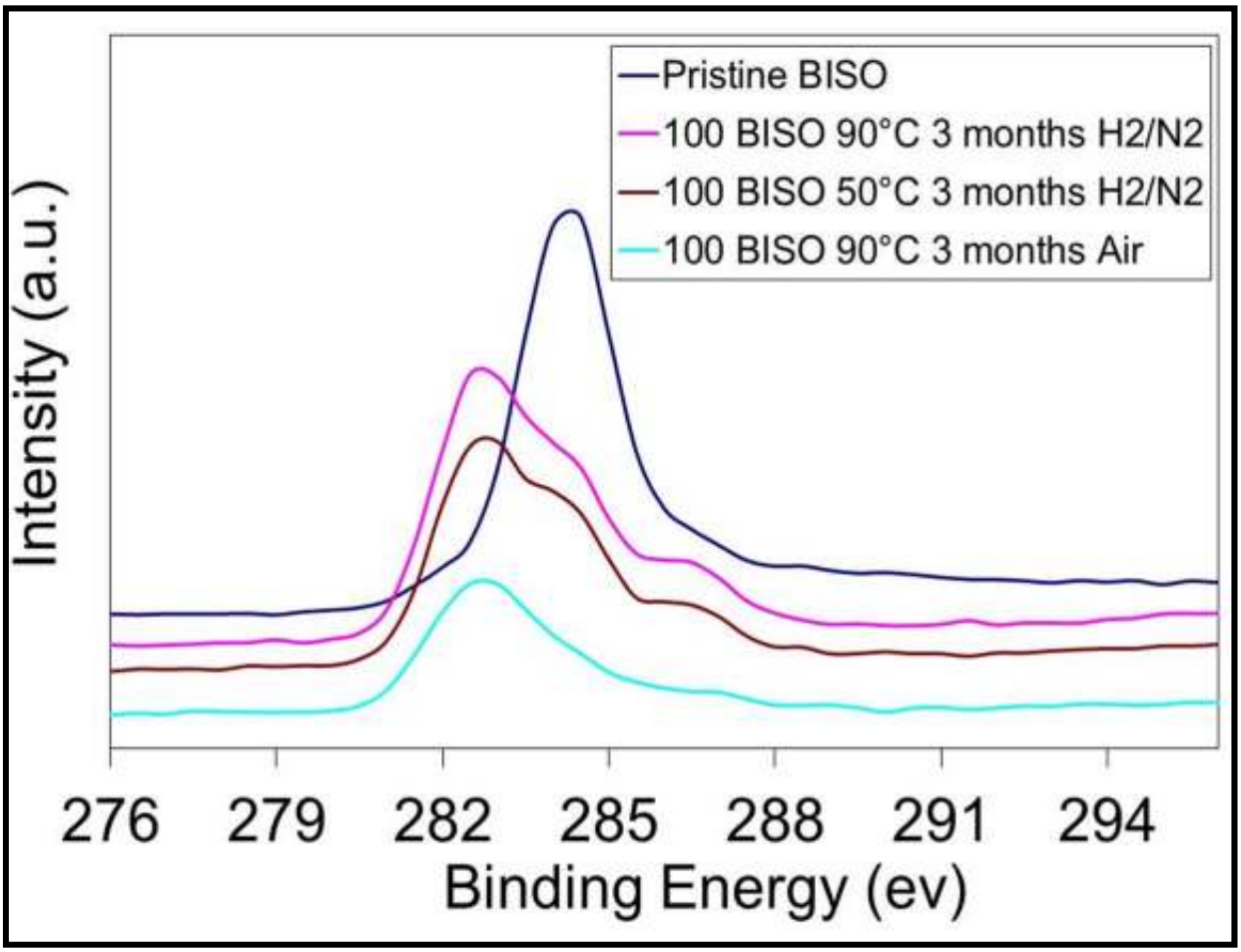

Fig. 32. *C_{1s} XPS spectra of BISO particles before and after 3 months of alteration at 50℃ and 90℃ under air and under reducing conditions.*

4.3.4. Implications for alteration rates

Alteration under oxygen atmosphere (air) leads to the increase of oxygen amount in the surface of particles. As can be seen from the data of EDX, EPMA and XPS, the corrosion of SiC and pyrocarbon is important under air compared to H_2/N_2 atmosphere.

The chemical analyses of the alteration solutions did not allow to derive alteration rates due to the precipitation of silica, and carbon is difficult to quantify due to volatilization. Furthermore, Information on the corrosion rate of SiC and pyrocarbon cannot be directly obtained from surface analysis with the used methods (EDX, XPS) due to the low alteration rates and the small alteration layer in the time frame of the experiments but we attempted to calculate a maximum rate using the quantitative EPMA data. From Table 7 the Si atomic concentration decreased from 48.5% to an average of 42.1% (6.4% decrease) after 3 months of alteration under air. This apparent decrease can reasonably be attributed to oxygen uptake due to the oxidation of Si to SiO_2 and likely to hydration water. Thus, we can reasonably consider that the altered percentage in the total analysed volume of SiC (1 μm^3) is 6.4×100/48.5 = 13.2%. Hence, if we consider the

total analysed thickness of 1 µm, the thickness of the altered SiC is 13.2/100 = 0.132 µm = 132 nm per 3 months giving a rate of 132/90 = 1.5 nm/d. This rate though is likely conservative remains orders of magnitudes lower than that obtained for the French nuclear waste glass, which is estimated to 4×10^{2} nm/d at 90°C [32]. Fachinger *et al.* [8] found corrosion rates of SiC in clay pore water at 90°C in the order of 7×10^{-3} nm/d, which is even lower than our data and could be explained by the difference in experimental conditions (pH, surface area of SiC, water composition).

Also, we calculated the corrosion rate of SiC under reducing conditions from data of Table 7 and we found a rate of 1.2×10^{-1} nm/d, which is one order of magnitude lower than that obtained under oxidizing conditions. This difference in the alteration rate is similar to that reported by Fachinger *et al.* [8] who found corrosion rates of HTR fuels at 90°C in oxidizing conditions (air and oxygen atmosphere) about ten times higher than under anoxic conditions (argon).

According to XPS analysis of TRISO particles altered at 90°C for 3 months under reducing conditions (Fig. 29) the spectra clearly show the original signature of SiC within the 5 nm analysed thickness. This allows us to suggest that the oxidized fraction of the analysed thickness is lower than 5 nm. Hence, the corrosion rate is estimated to be < 5 nm / 90 days = 5.5×10^{-2} nm/d. Under oxidizing conditions the signature of SiC disappeared from the spectrum in Fig. 29, suggesting a rate higher than 5.5×10^{-2} nm/d.

For BISO particles, the interpretation of XPS data was difficult but quantitative EPMA analysis did not show any oxidation under reducing conditions even after 1 year of alteration, in good agreement with Fachinger *et al.* [8] findings, which confirms the high stability of pyrolytic carbon in aqueous media.

5. Conclusions

Alteration of TRISO (SiC) and BISO particles in conditions simulating deep geological radioactive waste disposal in France (50, 90°C; synthetic clay water) showed high stability of SiC and pyrolytic carbon under H_2/N_2 atmosphere. Under oxidizing conditions the SiC alteration rate at 90°C is estimated between 5.5×10^{-2} nm/d and 1.5 nm/d, while under reducing conditions rate was one order of magnitude lower (from less than 5.5×10^{-2} nm/d to 1.2×10^{-1} nm/d). Under air at 90°C SiC oxidized into magnesium silicates clay-type minerals and SiO_2. Mg-Si clays are known for their good retention properties with respect radionuclides. In the context of high-level radioactive waste disposal in clay formations, long-term reducing conditions are expected to prevail, thus assuring high stability of HTR spent fuel. However, alteration of spent-fuel under oxidizing conditions cannot be excluded, in particular under early accidental failure of barriers systems and water intrusion. Under these conditions fuel oxidation could occur with oxygen remains introduced during galleries construction but also could be generated together with oxidizing radicals and molecules (e.g. $OH^{\bullet}$, H_2O_2) via

water gamma radiolysis. Hence, it is important to evaluate the impact of water gamma radiolysis of SiC and carbon stability.

Acknowledgments

SEM and XPS work has been performed at the Institut des Matériaux de Nantes (IMN). A special thanks to Johan Vandenborre for his help with XPS interpretation.

References

[1] Martin, D.G. Nucl. Eng. Des. 213 (2002) 241–258.

[2] Miller, G.K., Petti, D.A., Varacalle, D.J., Maki, J.T. J. Nucl. Mater. 295, (2001) 205–212.

[3] Slack, G.A. Phys. Rev. 127 (3) (1962) 694–701.

[4] J.S. Goela, L.E. Burns, R.L. Taylor, Appl. Phys. Lett. 64 (1994) 131.

[5] S.J. Xu, J.G. Zhou, B. Yang, B.Z. Zhang, J. Nucl. Mater. 224 (1995) 12.

[6] McEachern DW, Wu W, Venneri F. Nucl Eng Des, 251 (2012) 102-110.

[7] N. Kirch, H.U. Brinkmann, P.H. Brucher. Nucl. Eng. Des.121 (1990) 241-248

[8] J. Fachinger, M. Den Exter, B. Grambow, S. Holgersson, C. Landesman, M. Titov, T. Podruhzina, Nuclear Engineering & Design; 236 (2006) 543–554.

[9] J. Fachinger, M. Den Exter, B. Grambow, S. Holgerson, C. Landesmann, M. Titov, T. Podruhzina, , 2nd International Topical Meeting on High Temperature Reactor Technology, Beijing, China, Paper #B08, 2004

[10] W. Gray, Radioactive Waste Management and the Nuclear Fuel Cycle 3 (2) (1982) 137.

[11] H. Hirayama, T. Kawakubo, A. Goto, , Journal of the American Ceramic Society 72 (1989) 2049.

[12] W. Kim, H. Hwang, J. Park, W. Ryu, Journal of Material Science Letters 22 (2003) 581.

[13] Jr. C. Henger, A. Schemer-Kohrn, S. Pitman, D. Senor, J. Geelhood, C. Painter, Journal of Nuclear Materials 378 (2008) 9.

[14] R.E. Tressler, M.D. Meiser, T. Yonushonis, J. Am. Ceram. Soc. 59 (1976) 278.

[15] D.W. McKee, D. Chatterji, J. Am. Ceram. Soc. 59 (1976) 441.

[16] A. Vinsot, S. Mettler, Caracterisation de la composition de l'eau interstitielle du Callovo-Oxfordien, Experiences PAC. Rapport ANDRA.D.RP.ADPE.05.0870, 2007.

[17] Jiti Konta, Applied Clay Science 10 (1995) 275-335.

[18] D.L. Parkhurst and C.A.J. Appelo: User's guide to Phreeqc (version 2) A computer program for speciation, batch reaction, one-dimensional transport, and inverse geochemical calculations, 99-4259, Water-resources investigations Report, Denver, CO USA, (1999) 312 p.

[19] P. Fenter and N.C. Sturchio, Progress in Surface Science 77 (2004) 171.

[20] S. Kerisit and C. Liu, Environmental Science and Technology 43 (2009) 777.

[21] H.W. Shim, K.C. Kim, Y.H. Seo, K.S. Nahm, E.-K. Suh, H.J. Lee, and Y.G. Hwang, Appl. Phys. Lett. 70 (13), (1997) 1757.

[22] Y. Wang, D. C. Alsmeyer, R. L. McCreery, Chem. Mater., 2 (1990) 557-563.

[23] R. O. Dillon, J. A. Woollam, J.V. Katkanant, Phys. ReV. B, 29(6) (1984) 3482-3489.

[24] A. C. Ferrari, J. Robertson, Phys. ReV. B, 61 (20) (2000) 14095-14107.

[25] K.N. Dalby, H.W. Nesbitt, V.P. Zakaznova-Herzog, P.L. King, Geochimica et Cosmochimica Acta 71 (2007) 4297–4313.

[26] J.F. Moulder, W.F. Stickle, P.E. Sobol, K.D. Bomben, in: J. Chastain (Ed.), Handbook of X-Ray Photoelectron Spectroscopy, Perkin-Elmer Corporation, Eden Prairie, Minnesota, (1992).

[27] J.F. Moulder, W.F. Stickle, PE Sobol, KD Bomben, Handbook of X-ray photoelectron spectroscopy. Eden Prairie, Minnesota: Perkin–Elmer; 1992.

[28] “Photoemission in solids I” Ed. M. Cardona dn L. Ley p.13, Springer Verlag (1978).

[29] J.F. Zhao, P. Lemoine, Z.H. Liu, J.P. Quinn, and J.A. McLaughlin, J. Phys.: Condens. Matter 12 (2000) 9201.

[30] X.B. Yan, T. Xu, S.R. Yang, H.W. Liu, and Q.J. Xue, J. Phys. D: Appl. Phys. 37 (2004) 2416.

[31] D. Rosenthal, M. Ruta, R.Schlögl, L. Kiwi-Minsker, Carbon 48 (2010) 1835-1843.

[32] P. Jollivet, S. Gin, S. Schumacher, Chemical Geology 330–331 (2012) 207–217.